OFFICE OF NAVAL RESEARCH
875 N. RANDOLPH STREET, ARLINGTON, VA 22203

CONTACT

REPORT SUBMISSION
FY 2009

ONR DEPT. 33 SEA WARFARE AND WEAPONS

View Contract Report (Printable View)

Date: 7/24/2009

Fiscal Year 2009 Annual Report: N00014-08-1-1052

Last Modified: 7/24/2009 3:46:56 PM

Name: Robert Tuttle
Organization: SAGINAW VALLEY STATE UNIVERSITY
City/State/Country: University Center/MI/USA
Title: Associate Prof.
Zip Code: 48710
Phone: 989-964-4676
Fax: 989-964-2717
Email: rtuttle@svsu.edu
Website: http://www.svsu.edu/

Contract Information

Contract/Grant Number: N00014-08-1-1052
Contract/Grant Title: Solidification Based Grain Refinement in Steels
Program Officer: Richard Fonda

CO-PI Information

Number of Co-PIs: 0

Abstract

The overall research objective of this project is to determine suitable grain refiners for cast steels. The project hopes to identify possible phases to grow delta ferrite and austenite using current nucleation theory, crystallographic data, and thermodynamics. Through thermal analysis experiments the effectiveness of possible nucleating compounds will be verified. A series of tensile testing experiments will also be done to determine how grain refinement affects the as-cast properties of steel castings. Experimentation for evaluating the most effective methods of introducing grain refiners in an industrial setting are also being done. The result of these experiments will expand the knowledge base on steel solidification and grain refinement theory.

Technical Section

N00014-08-1-1052(2).doc

N00014-08-1-1052(1).ppt

Progress Statement

This project has completed all of its year one tasks, which were Tasks 1-4 of the proposal. The PI examined current castings for heterogeneous nuclei which could be purposely introduced. No obvious nuclei were found in castings deoxidized with aluminum; however, there were indications of TiN or complex TiN-sulfide inclusions which may have helped nucleate delta ferrite. Using current heterogeneous nucleation theory, crystallographic analysis, and thermodynamic calculations, multiple phases were identified to assist the nucleation of austenite or delta ferrite from liquid steel. Thermal analysis experiments were successfully completed to verify the ability of the identified materials to nucleate austenite or delta ferrite.

Technology Transfer

The PI conducted a set of experiments with a research team at Missouri S&T. This team has developed a new FeMnAl steel with support from the Army. In April, this new steel alloy passed the Army's P900 armor standard. In June, the PI conducted a set of thermal analysis experiments to determine if any of the compounds found so far could produce refinement. Powders that were found to nucleate austenite were used since the material is a fully austenitic material. Undercooling measurements and metallographic examination of the samples found no refinement was produced. The likely cause of this is that the FeMnAl alloy contains 30% Mn and 9% Al which likely changed the lattice parameter of the austenite formed. Further work would be needed to develop grain refiners specific to this steel alloy. The experiments did help the Missouri S&T team eliminate grain refinement as a possible mechanism for improved mechanical properties when cerium is added. Experiments at Missouri S&T had found a dramatic increase in impact toughness through the addition of cerium; however, the cause was not known.

Refereed Journal Articles

None entered

Books and Chapters

None entered

Technical Reports

None entered

Contributed Presentations

None entered

Patents

None entered

Honors

1. RUBY Award
   to: Dr. Robert Tuttle of Saginaw Valley State University
   from: 1st State Bank, Tri-City Magazine, and WNEM TV 5
   The RUBY Award recognizes young professionals who have reached success at an early age. The recipients represent a wide range of professions and enterprises including international, national and statewide corporations, local business, government, education, medical and not-for-profit business.

Related Sponsored Work

1. Determination of Macroinclusion Sources in the Steel Casting Process
   for: SVSU Foundation (5,300)
   from: July 2007 to: August 2009
   The purpose of this project will be to determine how and where inclusions form in the steel casting process. Inclusions in steel castings result in broken cutting tools, increased repair welding, and reduced mechanical properties. Most investigators have attributed reoxidation during the steel casting process as the major source of inclusions. Locating the casting process step where the majority of reoxidation happens will enable foundries to develop processing techniques that significantly reduce or eliminate reoxidation and prevent inclusion formation. To determine where reoxidation occurs, a series of samples and oxygen measurements will be taken at several points in the steel foundry process. The samples will be analyzed for inclusion content, morphology, and chemistry. Computer mold filling simulations conducted as part of this study will enable visualization of possible inclusion formation regions inside the mold cavity. Based on the results of this study, process improvements will be proposed and their impact quantified by the amount of repair welding done and the inclusion levels in finished parts. Reduction or elimination of inclusions will improve the profitability, competitiveness, and market opportunities for Saginaw area steel foundries.

2. Effect of Cooling Rate on Ductile Iron Properties
   for: American Foundry Society ($47,546)
   from: April 2008 to: July 2009
   There is not a large amount of information available to foundries and design engineers on how cooling rate effects mechanical properties. AFS has sponsored projects that have examined the 65-45-12 and 80-55-06 grades of ductile iron. This project will focus on determining how cooling rate effects properties in the 100-70-03 ductile iron grade. Additionally, the project will collect cooling curves from actual molds to properly correlate the changes in mechanical properties observed in this project and the previous projects.

3. Ultrasonic Testing Gage R&R Study
   for: American Foundry Society ($68,743)
   from: April 2008 to: January 2010
   As quality demands for steel castings continually increase, delivering the desired quality economically remains a challenge. Foundries have traditionally used radiography for quality testing. The reliance on this technique stems from its visual nature and historical precedent. For medium to large steel castings, radiography can become expensive. The expense results from the shielding, regulator requirements and acquisition cost of the highly radioactive source needed when penetrating six inches of steel. Ultrasonic testing (UT) can provide significant cost savings over radiography, because it has significantly fewer safety requirements and costs less than a high energy x-ray source. There is a strong need to determine the actual reliability of UT inspection and correlate it with current radiographic standards. Little data is available to scientifically evaluate this non-destructive evaluation technique. The goal of this project is to address both issues through a round robin style study.

ONR Statistics

Papers Published: 0
Papers In Press: 2
Books/Chapters: 0
Books/Chapters In Press: 0
Technical Reports: 0
Invention Disclosures: 0
Patents Awarded: 0
Patents Pending: 0
Presentations: 0
Contributed Presentations: 0
Degrees Granted: 0
Honors: 1
Co-PIs: 0
Women Co-PIs: 0
Minority Co-PIs: 0
Graduate Students (Total): 0
Women Graduate Students: 0
Minority Graduate Students: 0
Undergraduate Students (Total): 2
Women Undergraduate Students: 0
Minority Undergraduate Students: 0
Post Doctoral Students (Total): 0
Women Post Doctoral Students: 0
Minority Post Doctoral Students: 0

Solidification Based Grain Refinement in Steels

Dr. Robert Tuttle
Saginaw Valley State University

Objective:

1) Identify possible phases to grow delta ferrite and austenite using current nucleation theory, crystallographic data, and thermodynamics.
2) Experimentally verify the effectiveness of possible nucleating compounds.
3) Extend grain refinement theory and solidification knowledge through experimental data.
4) Determine structure property relationships for grain refiners.
5) Formulate processing techniques for using grain refiners in the steel casting industry.

TA cup on stand.

Approach:

Use current heterogeneous nucleation theory, crystallographic data, and thermodynamic predictions to identify possible heterogeneous nuclei. These nucleation materials are then used in a thermal analysis experiment to examine the reduction in undercooling and reduction in austenite grain size to confirm nucleation. Later experiments will be used to evaluate the improvement in the mechanical properties of various steel alloys. The goal is to determine how to use grain refiners to produce

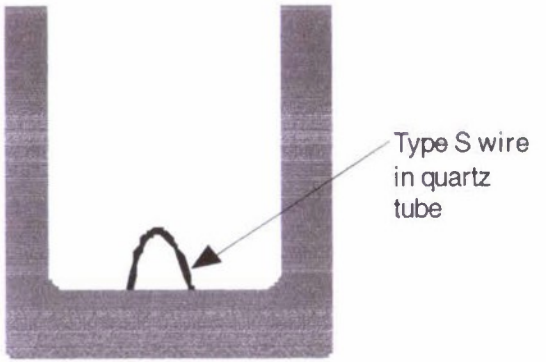

Sketch of TA cup.

20110929013

Solidification Based Grain Refinement in Steels

Dr. Robert Tuttle
Saginaw Valley State University

Recent accomplishments:

-Identified several possible grain refiners

-Conducted experiments which found useful grain refiners and reduction in grain size

Future Plans:

-Develop structure property relationships for grain refined steels

-Create industrially viable processing routes for grain refining steels for increased properties

-Expand current solidification knowledge in steels

1030 steel with no addition.

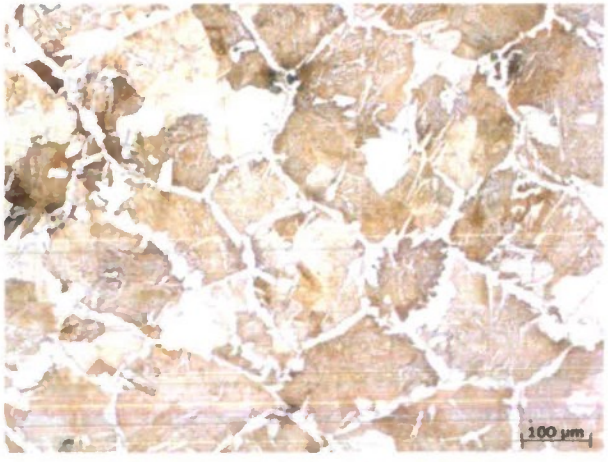

1030 steel with $CoAl_2O_4$ powder showing reduction in prior austenite grain size.

Progress Statement

This project has completed all of its year one tasks, which were Tasks 1-4 of the proposal. The PI examined current castings for heterogeneous nuclei which could be purposely introduced. No obvious nuclei were found in castings deoxidized with aluminum; however, there were indications of TiN or complex TiN-sulfide inclusions which may have helped nucleate delta ferrite. Using current heterogeneous nucleation theory, crystallographic analysis, and thermodynamic calculations, multiple phases were identified to assist the nucleation of austenite or delta ferrite from liquid steel. Thermal analysis experiments were successfully completed to verify the ability of the identified materials to nucleate austenite or delta ferrite.

Abstract

The overall research objective of this project is to determine suitable grain refiners for cast steels. The project hopes to identify possible phases to grow delta ferrite and austenite using current nucleation theory, crystallographic data, and thermodynamics. Through thermal analysis experiments the effectiveness of possible nucleating compounds will be verified. A series of tensile testing experiments will also be done to determine how grain refinement affects the as-cast properties of steel castings. Experimentation for evaluating the most effective methods of introducing grain refiners in an industrial setting are also being done. The result of these experiments will expand the knowledge base on steel solidification and grain refinement theory.

Technology Transfer

The PI conducted a set of experiments with a research team at Missouri S&T. This team has developed a new FeMnAl steel with support from the Army. In April, this new steel alloy passed the Army's P900 armor standard. In June, the PI conducted a set of thermal analysis experiments to determine if any of the compounds found so far could produce refinement. Powders that were found to nucleate austenite were used since the material is a fully austenitic material. Undercooling measurements and metallographic examination of the samples found no refinement was produced. The likely cause of this is that the FeMnAl alloy contains 30% Mn and 9% Al which likely changed the lattice parameter of the austenite formed. Further work would be needed to develop grain refiners specific to this steel alloy. The experiments did help the Missouri S&T team eliminate grain refinement as a possible mechanism for improved mechanical properties when cerium is added. Experiments at Missouri S&T had found a dramatic increase in impact toughness through the addition of cerium; however, the cause was not known.

TEXT AFTER THIS POINT WILL BE INCLUDED IN THE TECHNICAL SECTION OF THE ONLINE REPORT

Contract Information

Contract Number	N00014-08-1-1052

Title of Research	Solidification Based Grain Refinement in Steels
Principal Investigator	Dr. Robert Tuttle
Organization	Saginaw Valley State University

Technical Section

Technical Objectives

The overall research objective of this project is to determine suitable grain refiners for cast steels. Specific objectives are:

1) Identify possible phases to grow delta ferrite and austenite using current nucleation theory, crystallographic data, and thermodynamics.
2) Experimentally verify the effectiveness of possible nucleating compounds.
3) Extend grain refinement theory and solidification knowledge through experimental data.
4) Determine structure property relationships for the examined grain refiners.
5) Formulate processing techniques for using grain refiners in the steel casting industry.

Technical Approach

The wrought steel industry has successfully developed high strength low alloy (HSLA) grades of steel. Strength is developed in HSLA steels by thermomechanical grain refinement and precipitation hardening. This is achieved by precipitating niobium carbides, which pin the austenite grains and prevent grain growth during thermomechanical processing.[1-20] Strengthening is achieved by a Hall-Petch strengthening mechanism and precipitation hardening.[1-20] The thermomechanical grain refinement originally developed for these grades has also been adopted for other steel grades.[20] Unfortunately, steel castings cannot undergo thermomechanical grain refinement because they are produced near net shape. In many cases, steel foundries refine the structure of a casting through heat treatment. The energy required for grain refining via thermomechanical processes or heat treatment impacts the environmental friendliness and cost effectiveness of these grades. A better approach is to create a small grain structure by manipulating the solidification of steels. This will result in a processing route that both steel mills and steel foundries can use to improve properties. Also, alloys other than the traditional HSLA alloys, such as stainless steels, could be strengthened this way.

Solidification based grain refinement has been successfully employed in aluminum, copper, magnesium, and cast iron alloys. When metals solidify, there must be stable nuclei for grains to grow. There are two possible nucleation routes: homogenous nucleation, which requires a large amount of undercooling, and heterogeneous nucleation, which requires a foreign nuclei.[21] Homogeneous nucleation occurs in a metal when the melt has cooled enough to allow atomically small embryos to form in the melt. Formation of these embryos requires a significant driving force, because a high energy interface is created when they form. Heterogeneous nucleation occurs when new grains grow on foreign nuclei. Foreign nuclei are either introduced as a solid phase in the melt or as a phase that precipitates in the melt. To be effective, the foreign particle must remain solid long enough to nucleate a new grain, have a similar crystal structure to the desired phase, and have a favorable interfacial energy between the foreign particle and desired phase.[21-23] Unlike other metals, the melting temperature of steel makes it difficult to find a phase that has the required lattice parameter and a sufficiently high melting point to remain solid during solidification. Additionally, the solid state reactions that form ferrite, pearlite, and for some alloys, austenite make it difficult to identify the structure present just after solidification.

References

1. Zrnik, J., Kvackaj, T., Sripinproach, D., and Sricharoenchai, P., "Influence of plastic deformation conditions on structure evolution in Nb-Ti microalloyed steel", *Journal of Materials Processing Technology*, Vol 133, No 1-2, pp. 236-242, 2003.
2. Lottey, K. R., and Militzer, M., "Microstructure evolution in fine-grained microalloyed steels", *Materials Science Forum*, pp. 347-354, 2005.
3. Ghosh, A., Das, S., and Chatterjee, S., "Ultrahigh strength hot rolled microalloyed steel: Microstructure and properties", *Materials Science and Technology*, Vol. 21, No. 3, pp. 325-333, 2005.
4. Peter, J., Peaslee, K. D., and Panda, D. "Thermomechanical processing of HSLA wide-flange steel beams for increased core toughness", *Iron & Steel Technology*, Vol. 1, No. 7, pp. 172-180, 2004.
5. Fernandez, J.; Illescas, S.; Guilemany, J. M. "Effect of microalloying elements on the austenitic grain growth in a low carbon HSLA steel", *Materials Letters*, Vol. 61, No. 11-12, pp. 2389-2392, 2007
6. Chen, Guoan; Yang, Wangyue; Guo, Shouzhen; Sun, Zuqing. "Characteristics of microstructural evolution during deformation-enhanced ferrite transformation in Nb-microalloyed HSLA steel", *Journal of University of Science and Technology Beijing*, Vol. 14, No. 1,pp. 36-40, 2007.
7. Kang, J. S.; Huang, Y.; Lee, C. W.; Park, C. G., "Effect of thermo-mechanical process on the microstructure and mechanical properties of low carbon HSLA steels", *Advanced Materials Research*, Vol. 15-17,pp. 786-791, 2007.
8. Chakrabarti, Debalay; Davis, Claire; Strangwood, Martin, "Characterization of bimodal grain structures in HSLA steels", *Materials Characterization*, Vol. 58, No. 5,pp. 423-438, 2007.
9. Timokhina, I. B.; Hodgson, P. D.; Ringer, S. P.; Zheng, R. K.; Pereloma, E. V., "Precipitate characterisation of an advanced high-strength low-alloy (HSLA) steel using atom probe tomography", *Scripta Materialia*, Vol. 56, No. 7,pp. 601-604, 2007.
10. Hotta, S.; Murakami, T.; Narushima, T.; Iguchi, Y.; Ouchi, C., "Effects of cooling rate and direct hot deformation conditions after solidification on the austenitic microstructure evolved by simulated strip casting and thin slab casting processes in HSLA steels", *Advanced Materials Research*, Vol. 15-17,pp. 726-731, 2007.
11. Chen, Y. T.; Guo, A. M.; Wu, L. X.; Zeng, J.; Li, P. H., "Microstructure and mechanical property development in the simulated heat affected zone of V treated HSLA steels", *Acta Metallurgica Sinica*, Vol. 19, No. 1,pp. 57-67, 2006.
12. Megahed, Gamal; Paul, S. K.; Carboni, Andrea; Pigani, Alessandro; Piemonte, Carlo P., "The development of new steel grades and products: Casting and rolling of API X70 grades for arctic applications in a thin slab rolling plant", *Proceedings of the McMaster Symposium on Iron & Steelmaking*, Vol. 33,pp. 292-300, 2005.
13. Alvarez, P.; Lesch, C.; Bleck, W.; Petitgand, H.; Schottler, J.; Sevillano, J. Gil., "Grain refinement of rapid transformation annealing of cold rolled low carbon steels", *Materials Science Forum*, Vol. 500,pp. 771-778, 2005.
14. Lottey, K. R.; Militzer, M., "Microstructure evolution in fine-grained microalloyed steels", *Materials Science Forum*, Vo. 500,pp. 347-354, 2005.
15. Zarandi, Faramarz; Yue, Steve., "Improvement of hot ductility in the Nb-microalloyed steel by high temperature deformation", *ISIJ International* (2005), Vol. 45, No. 5,pp. 686-693, 2005.
16. Khoo, C. A.; Fourlaris, G., "Control of grain size by second phase particle additions in novel HSLA strip steels", *Material Science & Technology 2004*, Vol. 1, pp. 21-29, 2004.
17. Gao, Wen; Garcia, C. I.; DeArdo, A. J., "The nucleation of ferrite from a coarse grained austenite during the slow continuous cooling of an HSLA steel," *Mechanical Working and Steel Processing Conference Proceedings*, Vol. 41, pp. 243-256, 2003.
18. Zhao, X. M.; Wu, D.; Zhang, L. Z.; Liu, Z. Y., "Modeling of isothermal precipitation kinetics in HSLA steels and its application", *Acta Metallurgica Sinica*, Vol. 17, No. 6,pp. 902-906, 2004.
19. Beres, Miloslav; Weirich, Thomas E.; Hulka, Klaus; Mayer, Joachim., "TEM investigations of fine niobium precipitates in HSLA steel", *Steel Research International*, Vol. 75, No. 11,pp. 753-758, 2004.
20. Peter, Joerg; Peaslee, Kent D.; Panda, Dhiren., "Thermomechanical processing of HSLA wide-flange steel beams for increased core toughness", *Iron & Steel Technology*, Vol. 1, No. 7,pp. 172-180, 2004.
21. Wallace, J.F., "Grain Refinement of Steels", *Journal of Metals*, pp. 372-376, 1963.
22. Form, G.W., and Wallace, J.F.," Solidification of Metals: General Principals", *Transactions of the American Foundrymen's Society*, Vol. 68, pp. 145-156, 1960.

23. Turnbull, G.K., Patton, D.M., Form, G.W., and Wallace, J.F., "Grain Refinement of Steel Castings and Weld Deposits", *Transactions of the American Foundrymen's Society*, Vol 69, pp. 792-804,1961.

Progress Statement Summary

Tasks 1 through 4 were completed on schedule for this year. Microstructural examination of current production castings was carried out. No heterogeneous nuclei were identified in the castings deoxidized with aluminum. In castings deoxidized with titanium, TiN and titanium containing nitride-sulfide inclusions were observed at the center of prior austenite dendrites. TiN has been found in other work to act as suitable nuclei for delta-ferrite. Several materials were identified as possible nuclei for austenite and delta-ferrite. Identification of these materials was based on crystallographic similarity and thermodynamic predictions on their stability. Thermal analysis experiments were then done to determine if the selected phases actually acted as nuclei. Nucleation was confirmed based on the reduction of undercooling to start solidification and the reduction in grain size observed.

Next year, the project will focus on determining mechanical properties and grain refiner addition techniques. The thermal analysis experiments already conducted did not provide data on the improvement in mechanical properties. Their purpose was simply to assist in confirming what materials caused refinement. A series of experiments will be done to determine how grain refinement affects yield strength, ultimate tensile strength, and elongation. The experiments will consist of pouring tensile bars in a green sand mold and then tensile testing them. Several different alloys will be experimented with to determine which produces the most beneficial results. The second set of experiments to be done this year will be to look at the best methods of adding the grain refiner to a steel casting. At this time, the PI has not decided what these experiments will consist of. It is likely they will consist of different addition strategies for producing tensile bar castings.

Progress

A short synopsis of the work done during this year follows. The first section summarizes the work done on examining current production castings for heterogeneous nuclei. The second section presents the results of some of the thermal analysis experiments. At this time, the PI is working to publish results from this year to the open literature. As papers are accepted for publication, the PI will forward them to the program officer.

Examination of Steel Castings for Nucleation Phases

Examination Procedure

Samples from three local foundries were acquired for examination without undergoing any heat treatment. The foundries were selected in an attempt to gain a broad selection of alloys and processes. Sample 1 was a section of 8620 steel gating from a local investment casting company. The foundry melts using a 500 lb (225 kg) high frequency induction furnace and deoxidizes with aluminum. Samples 2, 3, and 4 were cast parts from a resin bonded sand foundry which melts with a 2,000 lb high frequency induction furnace and deoxidizes using titanium. A cover made from 1030 steel was Sample 2. Sample 3 was an outrigger component also poured from 1030 steel. A small hinge poured from 4140 steel was selected for Sample 4. The last foundry supplying samples produces large (over 14 ton) steel castings by resin bonded molds and an electric arc furnace. Aluminum is used for deoxidation. For this foundry, a sample was acquired from the steel stream during tapping. Samples 5 and 6 were a 1 inch diameter, 6 inch long bar. Sample 5 was a slightly modified 1050 steel. An ASTM A148 Grade 105-85 steel made Sample 6. The chemistries for all the samples are listed in Table 1.

Table 1 Chemistries for each sample examined.

Sample	C(wt.%)	Mn(wt.%	Si(wt.%)	Cr(wt.%)	Ni(wt.%)	Mo(wt.%)	P(wt.%)	S(wt.%)

		)						
1	0.18	1.00	0.80	0.45	0.50	0.21	0.035	0.030
2,3	0.29	.95	0.98	0.32	0.48	-	0.030	0.032
4	0.44	0.80	0.77	0.85	0.40	0.22	0.036	0.030
5	0.40	0.96	0.47	0.98	0.25	0.40	0.034	0.022
6	0.28	0.96	0.40	0.62	0.90	0.27	0.032	0.029

All of the castings were sectioned into several metallurgical mounts for analysis. Each was ground using standard metallographic practice. The samples were then rough polished with 6 μm and 1 μm diamond paste. Final polishing was done with 0.05 μm alumina. To assist with locating possible nucleation sites, the samples were etched by immersing the sample in a saturated aqueous picric acid solution for five minutes in an ultrasonic bath to reveal the prior austenite boundaries. Optical microscopy was conducted to examine the as-cast structure. After carbon coating, a scanning electron microscope (SEM) with an energy dispersive spectrometer (EDS) was employed to look for inclusions within the prior austenite structure and determine their chemical analysis.

Results

Optical Microscopy

For most of the samples, the etching successfully revealed the prior austenite boundaries. One drawback to sat. aq. picric acid is that it does not always reveal the prior austenite boundaries.[1,2] However, this is the most common method.

Figure 1 Etched microstructure of Sample 1.

The etched structure of Sample 1 only reveals the room temperature structure of proeutectoid ferrite, acicular ferrite, and small amounts of pearlite (See Figure 1). No evidence of the as-cast austenite dendrite structure was observed. The gating system for this sample resides at the thermal center of the casting. Therefore, the cooling rate was relatively slow. As Sample 1 cooled, the austenite dendrites would have grown into larger equiaxed grains. The shape and size of these equiaxed grains can be seen by the distribution of proeutectoid ferrite. Upon

further cooling, the proeutectoid ferrite formed at the austenite grain boundaries; the boundaries act as nucleation points for ferrite formation.[1] The slow cooling rate also provided time for any carbon segregation to equalize throughout the part. Cooling through the eutectoid temperature, a small amount of pearlite formed near the proeutectoid ferrite and the acicular ferrite formed. The formation of acicular ferrite was likely due to the actual cooling rate experienced and the large size of the austenite grains. The cooling rate appears to have been sufficiently fast to allow the formation of acicular ferrite but not a completely pearlitic matrix. The large diffusion distance due to the austenite size would have also driven the formation of acicular ferrite instead of pearlite. Because the relationship between any possible nucleating inclusions and the as-cast structure could not be discerned, it was not possible to further examine this sample.

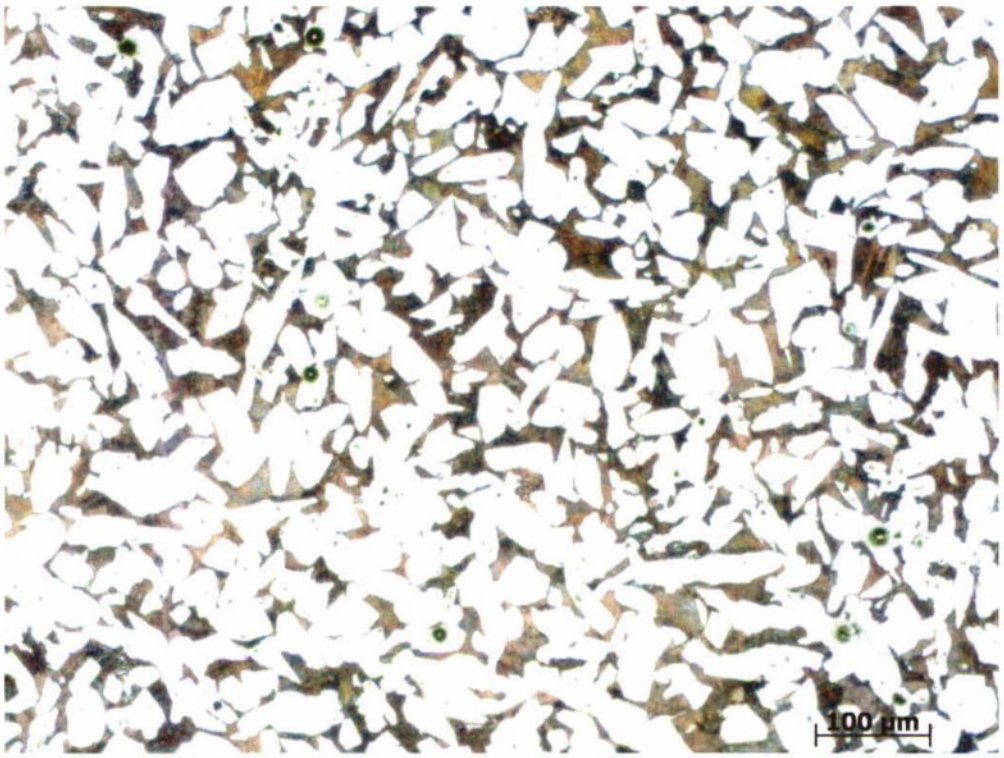

Figure 2 Micrograph of structure from Sample 2.

It is very difficult to discern the as-cast structure in Sample 2 (See Figure 2). However, close examination of ferrite grain clusters provided an indication of the past dendritic structure. Some of the ferrite clusters had a structure that exhibits some branching from a central line, similar to a dendrite. The reader may wonder why examining the structure of ferrite clusters would provide an indication of as-cast structure. While the casting solidifies, carbon tends to be rejected into the liquid at the solid/liquid interface due to limited diffusion in the solid. The limitation on diffusion in the solid could be due to the actual temperatures involved or more likely, the speed with which the solidification front progresses through the liquid. Since the liquid at the solid-liquid interface enriches in carbon, the carbon content in the dendrite changes with time. The center of the dendrite will be low in carbon while the exterior of the dendrite will be carbon rich, if there is insufficient time or the diffusivity of carbon is low due to temperature this segregation will not equalize. Any carbon not incorporated into the already solidified material will concentrate in the remaining liquid; therefore, the last areas to solidify are carbon rich. Depending on the cooling rate, the carbon may or may not have the ability to diffuse throughout the microstructure of the sample. The microstructure in Figure 2 would indicate that the cooling rate was fast enough to the prevent carbon redistribution and dendrite coarsening that was observed in Sample 1. When Sample 2 cooled through the eutectoid reaction, the carbon gradient in the microstructure allowed the proeutectoid ferrite to form at the center of the austenite dendrites because these were low in carbon. The lower carbon concentration at the center made ferrite formation easier since there was less carbon to be rejected into the remaining microstructure. Once the sample underwent the eutectoid reaction, the carbon rich regions transformed to pearlite. This sample was further examined under the SEM for possible nucleating phases.

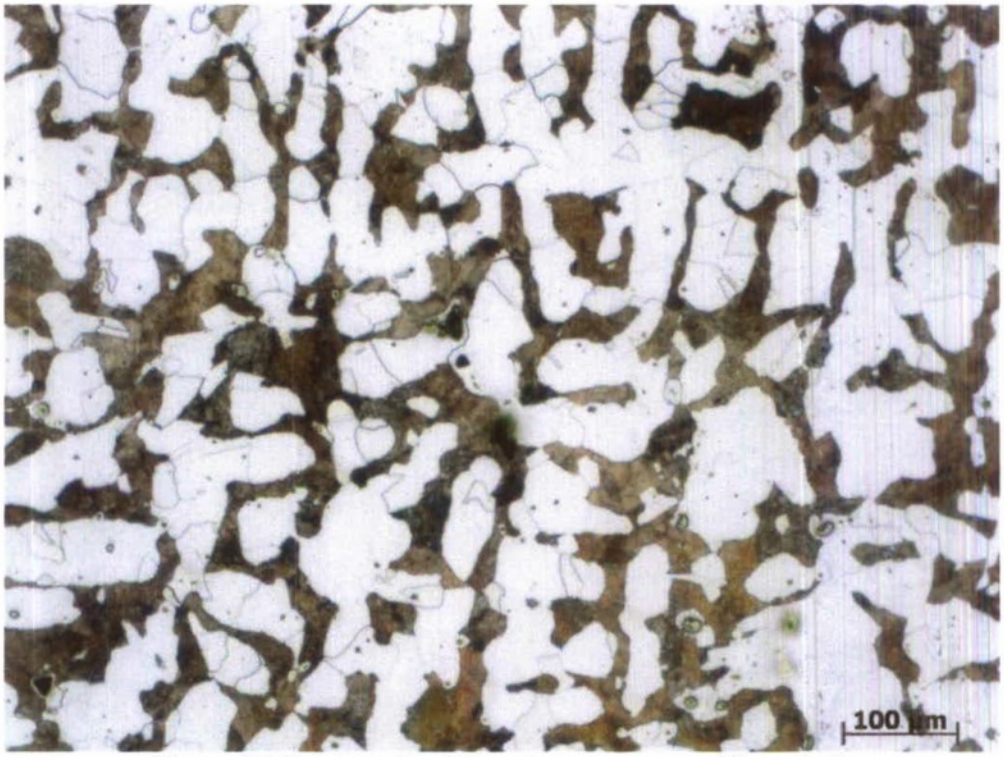

Figure 3 Micrograph of the microstructure of Sample 3.

Due to the larger size of this casting and therefore the slower cooling rate, the dendritic structure is much coarser in Sample 3 (See Figure 3). Unlike Figure 2, the dendritic structure of the ferrite clusters can be easily discerned. The carbon segregation during solidification, which was explained in the previous paragraph, created a low carbon region within the austenite dendrites. When the casting cooled, the proeutectoid ferrite had an easier time forming at the center of the dendrites. The distribution of the proeutectoid ferrite preserved the as-cast dendritic structure.

It was impossible to determine the as-cast structure of Sample 4 (See Figure 4). Unfortunately, the sat. aq. picric acid etch did not produce sufficient contrast between the ferrite/pearlite structure of the casting or the prior austenite boundaries. Other authors have noted a lack of response periodically to this etch for revealing prior austenite grain boundaries.[1,2] As a result, Sample 4 was not examined any further.

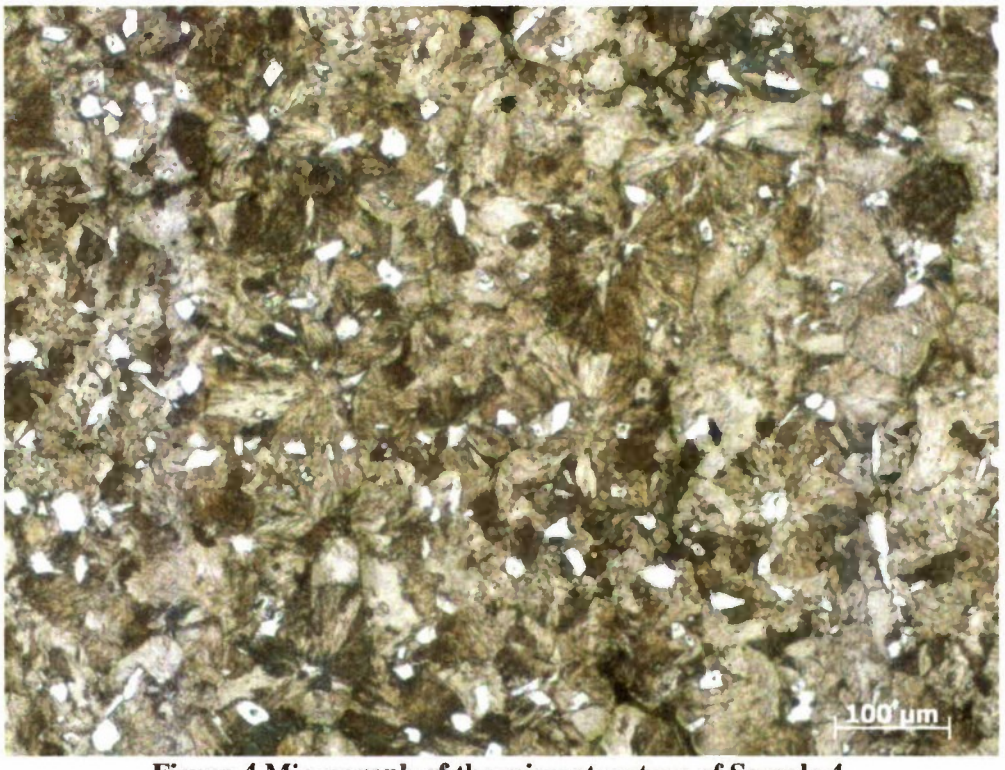

Figure 4 Micrograph of the microstructure of Sample 4.

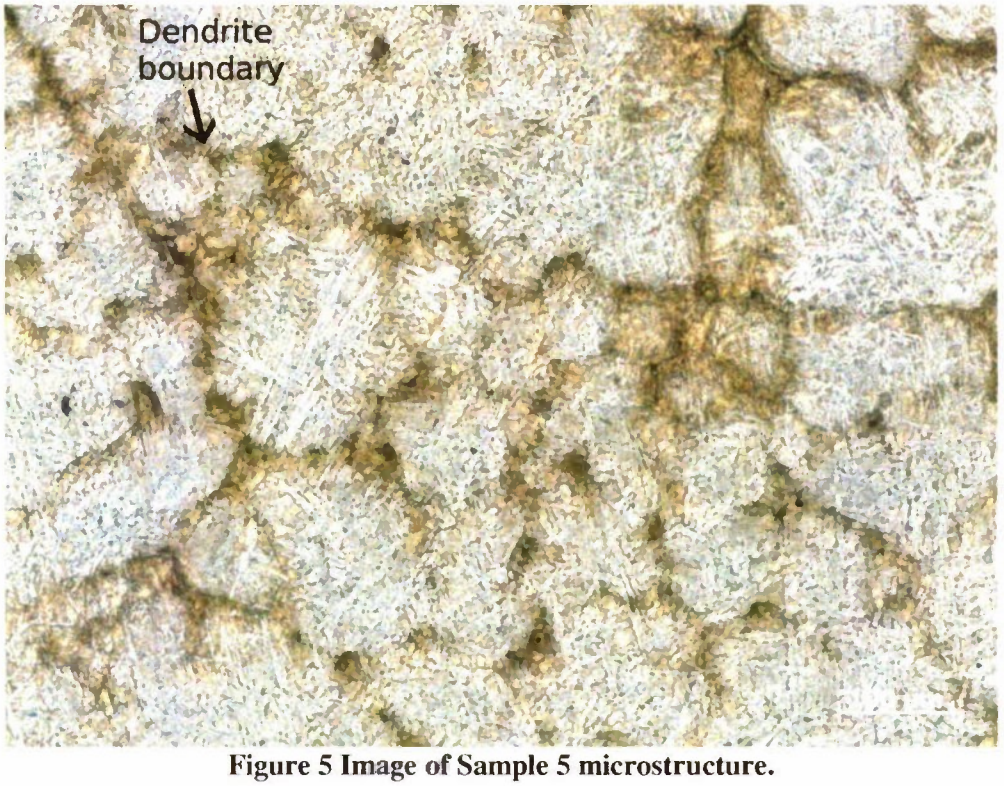

Figure 5 Image of Sample 5 microstructure.

The prior austenite structure of Sample 5 is visible in Figure 5. It is difficult to resolve the structure due to the acicular ferrite structure dominating the sample contrast. The dark areas within Figure 5 are the prior austenite dendrite boundaries.

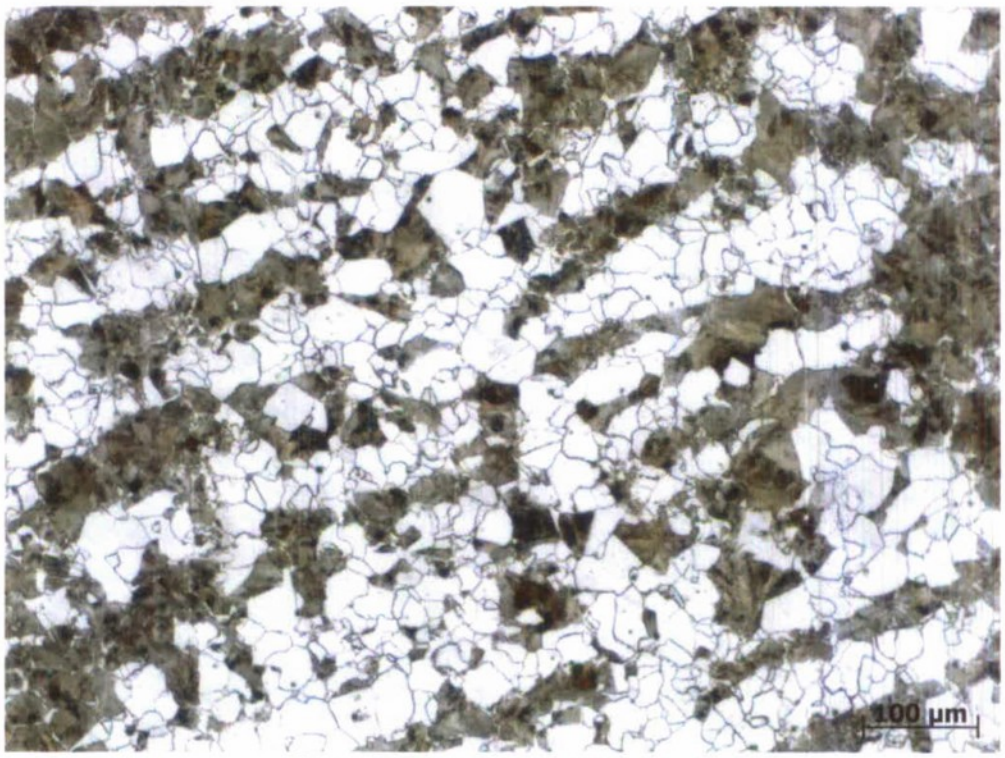

Figure 6 Micrograph of Sample 6.

The dendritic structure is clearly evident in this material due to the distribution of ferrite grains which preserved the austenite dendrite structure (See Figure 6). Interestingly, Sample 6 appears to have the largest dendrite size of all the samples.

Electron Microscopy

Samples 2,3,5 and 6 were further examined using the SEM. Inclusions found within dendrites were analyzed with EDS spectroscopy to assist with identifying the phase. One of the difficulties with searching for nucleating phases using only optical microscopy and an SEM is that crystallographic information cannot be found. Because some of the inclusions are engulfed by the solidification front and others may be possible nucleation sites, crystallographic information is needed. Ideally, such an investigation should include transmission electron microscopy (TEM) to capture crystallographic relationships between inclusions and austenite. But, the alloys analyzed did not contain retained austenite that could be examined to determine the crystallographic relationship between the austenite dendrites and a particular inclusion. The microstructure that encased the inclusions has gone through the eutectoid reaction and likely lost the crystallographic relationships of the as-cast structure.

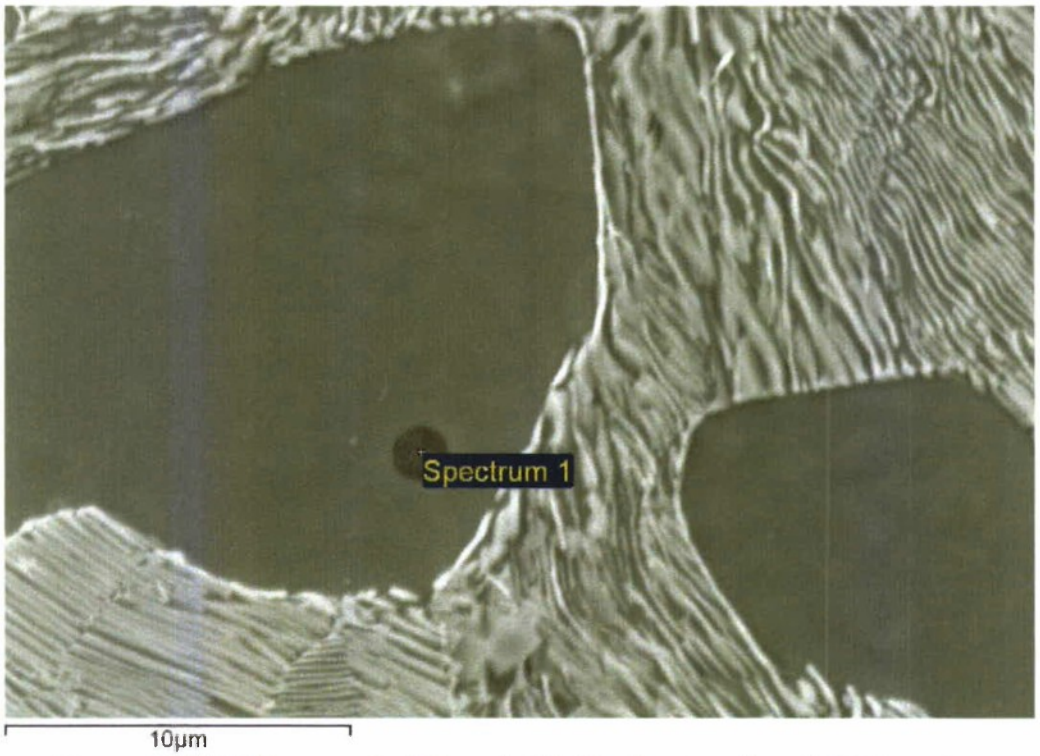

Figure 7 SEM Micrograph of Sample 2 indicating location of EDS spectra.

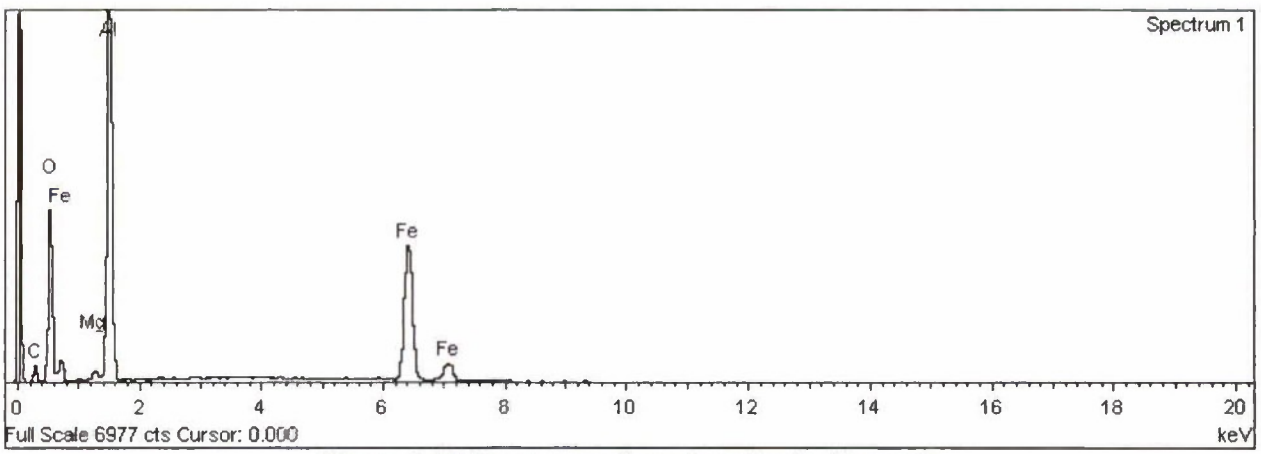

Figure 8 EDS spectrum from location in Figure 7.

Figure 7 is an inclusion near the tip of a prior austenite dendrite tip in Sample 2. The chemical analysis was consistent with alumina (See Figure 8). Due to its location at the tip of a dendrite, this particle was probably engulfed during solidification and did not serve as a nucleating site. Titania, iron oxides, and silicates were also observed within these dendrites. The most interesting finding within this sample was a small particle near the center of a dendrite (See Figure 9). The chemical analysis is consistent with TiN (See Figure 10).

Figure 9 Particle near the center of a prior austenite dendrite in Sample 2.

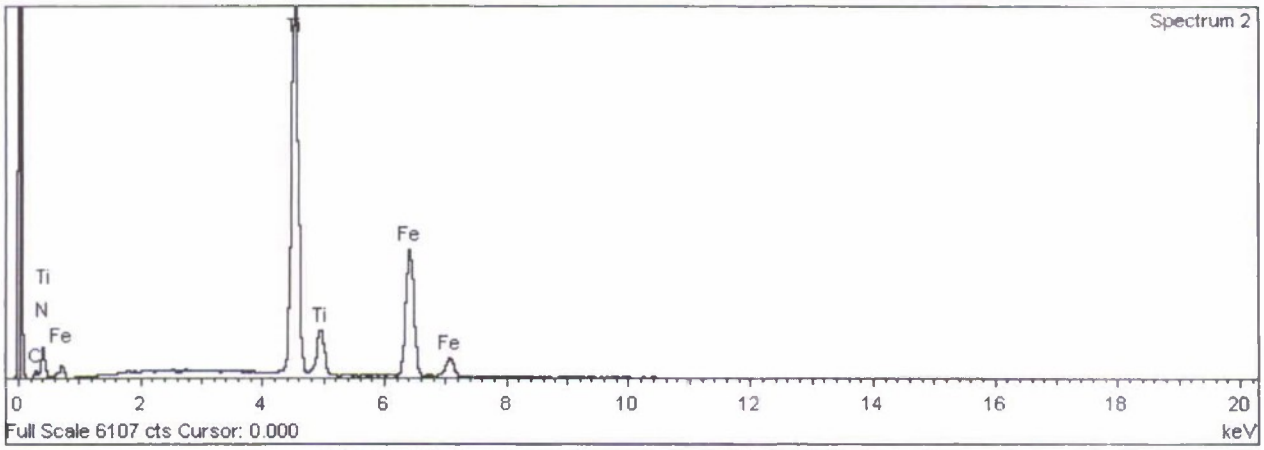

Figure 10 Spectrum from the particle in Figure 9.

Figure 11 SEM image of Sample 3.

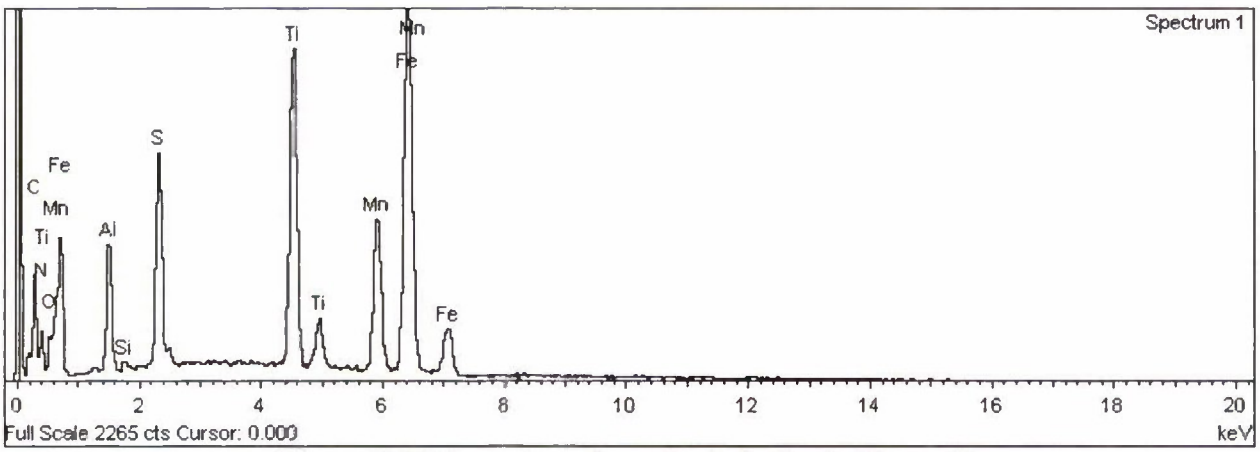

Figure 12 EDS spectrum from the inclusion in Figure 11.

While the inclusions did not appear very different in Sample 3, the inclusions frequently had more complicated chemistries (See Figure 11 and 12). The analysis in Figure 12 could be explained if the inclusion is actually an agglomeration of oxides, sulfides, and nitrides. A definite conclusion could not be provided as to the actual phase formed since crystallographic data was not captured. The author also noticed other inclusions composed primarily of manganese, titanium, and sulfur. These spectra were not included to space limitations.

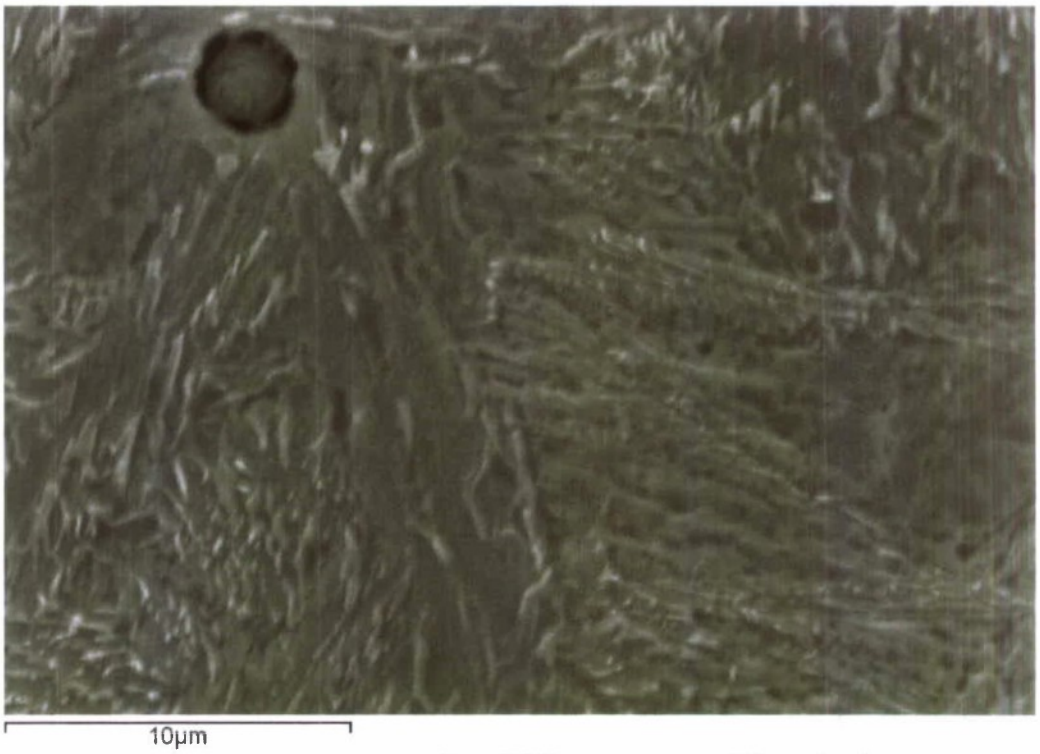

Figure 13 Representative SEM micrograph of Sample 5.

It was impossible to differentiate the prior austenite boundaries from the acicular structure of Sample 5 (See Figure 13). The SEM primarily generates its image from topological changes in the sample when using a secondary electron detector.[3] The topological signal created by the acicular ferrite structure seems to have over powered any signal generated by the prior austenite boundaries. Therefore, it was impossible to determine how inclusions were related to the as-cast structure in Sample 5.

The structure of Sample 6 under the SEM is presented in Figure 14. The author was not able to easily determine any possible nucleation sites. Most of the inclusions observed had compositions typical for furnace slag and appeared at the outer regions of the prior austenite dendrites. These inclusions were likely engulfed during solidification. Their location within the microstructure does not suggest that they served any function in developing the as-cast structure.

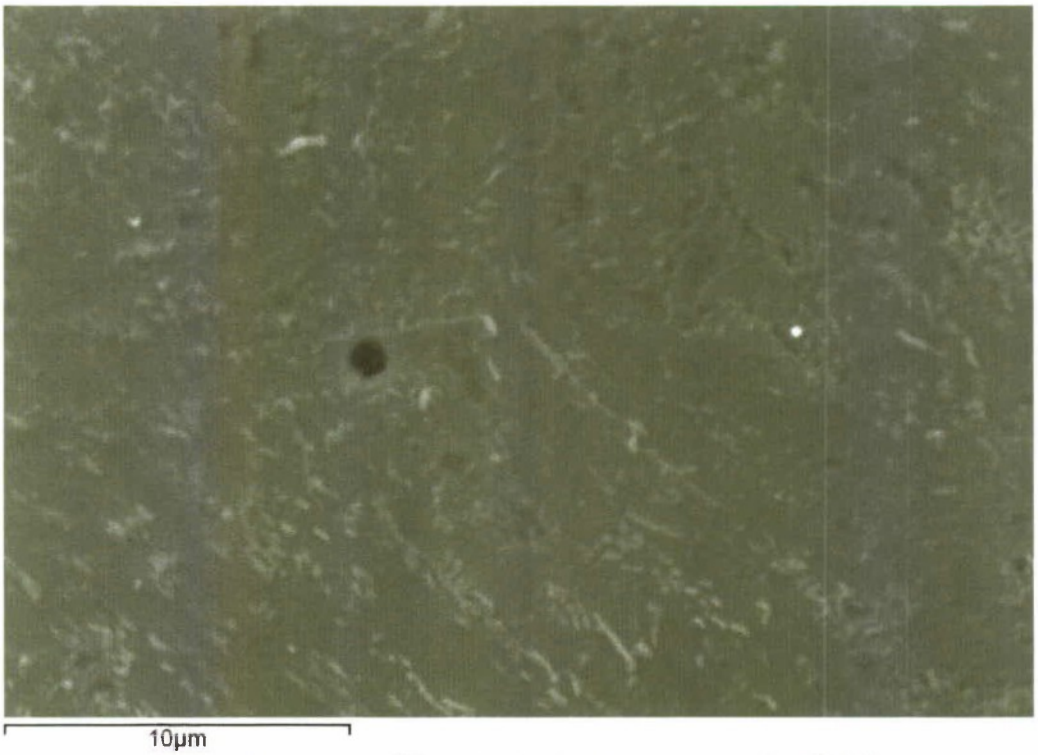

Figure 14 Image of Sample 6 microstructure under SEM.

Crystallographic Analysis

Based on the observations from the SEM investigation, three materials were evaluated for crystallographic comparisons with austenite and δ-ferrite. For a material to act as an effective heterogeneous nucleation site, it must be solid at the steel's solidification temperature, stable within liquid steel, and be wetted by the steel.[4,5,6] The first two criteria can be confirmed by looking at material references and through thermodynamic calculations. Obtaining wetting data to determine if liquid steel will wet the material is very difficult. The lack of data is due to the difficulty in performing wetting studies with liquid steel. Instead of using wetting data, most researchers examine the lattice disregistry between the solidifying phase and the proposed nucleation phase. This is because metals are more likely to wet another material as the crystal structure of the material becomes similar to the solidified metal. The most general way to calculate lattice disregistry between two similar crystal structures is with the Bramfit's modification to the Turnbull-Vonegut equation (See Equation 1).[6]

$$\delta_{(hkl)n}^{(hkl)s} = \sum_{i=1}^{3} \frac{\left| d_{[uvw]_s^i} cos\theta - d_{[uvw]_n^i} \right|}{d_{[uvw]_n^i}} \Big/ 3 \; X100 \qquad (1)$$

where, (hkl)s = a low-index plane of the substrate, [uvw]s = a low-index direction in (hkl)s, (hkl)n = a low-index plane in the nucleated solid, [uvw]n = a low-index direction in (hkl)n, $\delta_{(hkl)n}^{(hkl)s}$ = disregistry between (hkl)s and (hkl)n planes, $d_{[uvw]n}$ = the interatomic spacing along [uvw]n direction, $d_{[uvw]s}$ = the interatomic spacing along [uvw]s direction, and θ = the angle between the [uvw]s and [uvw]n directions.

Table 2 lists the disregistries between each material and austenite. It is fascinating that, while TiN and TiC have the lowest disregistries, they are not as low as is generally agreed on from other alloys for nucleation.[4-6] However, analyzing the disregistry between TiN and TiC and δ-ferrite reveals a much closer correlation (See Table 3). These results are in agreement with Bramfitt's earlier work.[6]

Table 2 Lattice parameters and calculated disregistries with austenite.[7]

Material	Unit Cell	Pearson Symbol	Lattice Parameter (nm)	Disregistry (%)
TiO_2	Rutile	tP6	0.4592	26
TiN	Rock Salt	cF8	0.4240	16
TiC	Rock Salt	cF8	0.4327	17
Austenite	FCC	cF4	0.3648	-

Table 3 Disregistries between selected phases and δ-ferrite and their cyrstallographic infomration.[7]

Material	Unit Cell	Pearson Symbol	Lattice Parameter (nm)	Disregistry (%)
TiO_2	Rutile	tP6	0.4592	56
TiN	Rock Salt	cF8	0.4240	4.5
TiC	Rock Salt	cF8	0.4327	6.8
δ-ferrite	BCC	cI2	0.2866	-

The reader might at first notice that the lattice parameters of TiN and TiC are much larger than δ-ferrite's. But, the calculated disregistry is very low. In both cases, the disregistry between the two and δ-ferrite are calculated based on the distance between the titanium atoms in the unit cell and not the entire length of the unit cell (See Figure 15). While only TiN inclusions were observed, the lattice disregistry analysis does point to the possibility of TiC inclusions acting as nuclei. This was observed in Wallace's early work.[8-10] It is possible that TiC inclusions were not detected because of the carbon coating placed on the sample for the SEM investigation.

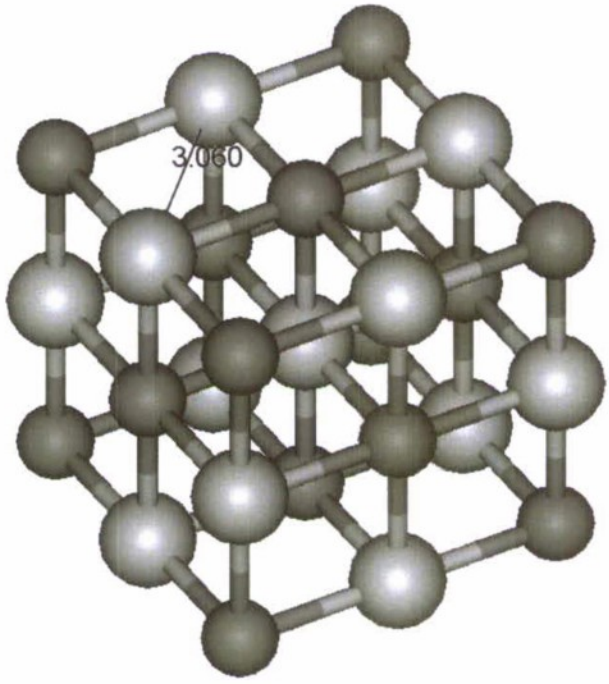

Figure 15 Crystal structure of TiC depicting the measurement of space between Ti atoms (Ti -light grey and C –dark grey).

Using the steel chemistry for Samples 2 and 3, thermodynamic calculations were conducted using ThermoCalc© to predict the phases formed during solidification. δ-ferrite is predicted to begin forming at 1494°C while austenite would not begin forming until 1475°C. The alloy is predicted to finish solidifying at 1415 °C. Therefore, it is possible that TiN inclusions could assist the nucleation of δ-ferrite dendrites which later went through a solid state transformation to austenite. It was these austenite dendrites that were then observed in Samples 2 and 3.

Conclusions

Several commercial castings were examined for possible nucleation sites. Through optical and electron microscopy, inclusions were detected at the center of prior austenite dendrites. TiN particles were found in two of the samples. Titanium nitride has a good crystallographic match to δ-ferrite and could have nucleated some of the primary dendrites. Thermodynamic predictions indicate that δ-ferrite forms before austenite in the steel alloy used to produce those samples. While not detected, TiC also appears to be a likely phase. It should be possible to purposely add TiN to reduce the grain size of castings leading to improved mechanical properties. Future testing will be required to confirm that TiN or TiC effectively nucleate delta ferrite.

References

1. Krauss, G., *Steels: Processing, Structure, and Performance*, pp 121, ASM International, Materials Park, OH (2005).
2. Vander Voort, G. F., *Metallography: Principles and Practice*, pp 218, McGraw-Hill, New York (1984).
3. Goldstein, J., *Scanning Electron Microscopy and X-ray Analysis: A text for Biologists, Materials Scientists, and Geologists*, 2nd ed., pp 88, Plenum Press, New York (1992).
4. Campbell, J., *Castings*, 2nd ed., pp 167, Elsevier Butterworth Heinemann, Oxford (2003).
5. Gruzleski, J. E., *Microstructure Development During Metalcasting*, pp 48, American Foundry Society, Schaumburg, IL (2000).
6. Bramfitt, B. L., "The Effect of Carbide and Nitride Additions on the Heterogeneous Nucleation Behavior of Liquid Iron," *Metallurgical Transactions*, vol. 1, pp 1987-1995 (1970).
7. Villars, P., *Pauling File*, 1995, http://crystdb.nims.go.jp/, (2 March, 2009).
8. Turnbull, G.K., Patton, D.M., Form, G.W., and Wallace, J.F.,"Grain Refinement of Steel Castings and Weld Deposits", *Transactions of the American Foundrymen's Society*, Vol 69, pp 792-804 (1961).
9. Wieser, P.F., Wallace, J.F., and Church, N., "Grain Refinement of Steel Castings", *Journal of Metals*, vol. 19, pp 44-51 (1967).
10. Church, N., Wieser, P., and Wallace, J.F., "Control of Cast Grain Size of Steel Castings, Effect of Refinement on Properties", *Modern Castings*, Vol 49, pp 129-144 (1966).

Plain Carbon Steel Thermal Analysis Experiments

Grain refinement is based on heterogeneous nucleation theory. To be an effective nuclei, the nucleating phase must satisfy three conditions: 1) be solid at the liquidus temperature of the metal; 2) remain stable in the liquid; and 3) the particle must have low lattice disregistry with the solid metal.[1-6] Lattice disregistry (δ) for crystal structures identical to the host metal can be computed by taking the difference in lattice parameters of the two unit cells. However, there are crystal structures that share atom placement on different planes. The best example of this is the atom spacing on the (111) plane in the face center cubic (FCC) unit cell matches the basal planes of the hexagonal closed packed (HCP) unit cell. Determination of the lattice disregistry for similar crystal structures requires the use of the Bramfitt's modified Turnbull-Vonnegut equation:

$$\delta_{(hkl)_n}^{(hkl)_s} = \sum_{i=1}^{3} \frac{\left| \left(d_{[uvw]_s^i} \cos\theta\right) - d_{[uvw]_n^i} \right|}{d_{[uvw]_n^i}} * 100$$

Equation 1

where, $(hkl)_s$ = a low-index plane of the substrate, $[uvw]_s$ = a low-index direction in $(hkl)_s$, $(hkl)_n$ = a low-index plane in the nucleated solid, $[uvw]_n$ = a low-index direction in $(hkl)_n$, $d_{[uvw]n}$ = the interatomic spacing along $[uvw]_n$, $d_{[uvw]s}$ = the interatomic spacing along $[uvw]_s$, and θ = the angle between the $[uvw]_s$ and $[uvw]_n$.[6]

This series of thermal analysis experiments on 1010 and 1030 steel were conducted to evaluate the nucleation potential of theoretically selected materials. Materials were chosen based on their low lattice disregistry with either δ-ferrite or austenite. Powders of these materials were added in the thermal analysis (TA) cups and the solidification cooling curve recorded. Cooling curve analysis and microstructural examination were used to determine if refinement occurred.

EXPERIMENTAL PROCEDURE

A series of thermal analysis experiments were conducted to determine the effectiveness of selected phases for acting as heterogeneous nuclei for steel. The nucleating compounds were selected based on their crystallographic structure, lattice disregistry, and thermodynamic stability in liquid steel. Twenty three kilograms of steel was melted in a high frequency induction furnace for each experimental run. The charge material consisted of clean 1010 or 1020 steel punching. Table 1 lists the average chemical analysis for each steel grade.

Table 4 Average Chemical Analysis of Each Steel

Sample	C (wt. %)	Si (wt. %)	Mn (wt. %)	P (wt. %)	S (wt.%)	Al (wt. %)
1010	0.14	0.41	0.18	0.009	0.0085	0.12
1030	0.34	0.52	0.36	0.016	0.005	0.045

Once at 1650°C, an oxygen probe was used to determine the oxygen content of the melt. Aluminum wire was added to fully deoxidize the melt and achieve a 0.04% residual aluminum amount. Graphite was also added to meet the target carbon content of the grade. Once the heat was deoxidized, a chemical sample was taken. The furnace was tapped into a small hand ladle that then poured a small amount of steel into a TA cup. Ten TA cups were poured for each run. The first and last TA cups contained no addition in them. This allowed the author to determine if the steel decarburized or otherwise changed during the run. The second through eight TA cups had 5g of the selected powder in them before the steel was poured. The pour order of these cups was fully randomized. Placing powder in the TA cups ensured no cross contamination of the powders. For the 1010 heats, NiAl, W, TiC, and TiN were selected because of their excellent crystallographic matching with δ-ferrite. TiO_2, and CeO_2 were also added in these runs as additional controls. NbC, MgO, La_2O_3, and AlN were chosen for the 1030 heats for their similarity to the crystal structure of austenite. CeO_2 was also added in these runs as a control. Due to its use by investment casting foundries for refinement, $CoAl_2O_4$ powder was also added. All the powders were high purity, -325 mesh powders. Three replicates per powder and alloy were done. As each cup solidified, a computer data acquisition system recorded the temperature as a function of time.

The cups were made from shell core sand with a single Type S thermocouple at the bottom (See Figure 1). The thermocouple wire was contained in a small quartz tube. Each cup was placed on a stand which was then connected to a computer for data acquisition (DAQ) (See Figure 2). Temperature readings were acquired at a rate of ten samples per second. After acquisition, the data was exported and analyzed in a spreadsheet program.

Each TA sample was sectioned and examined in optical microscopy. The samples were ground with SiC paper in the order of 240, 320, 400, and 600 grit. Initial polishing was done with 6μm and then 1μm glycol suspended diamond compounds before a final polish with 0.05 μm alumina. Ultrasonic cleaning for five minutes with an organic soap was done between the diamond polishing stages and the alumina polish. The samples were etched with 2% nital.

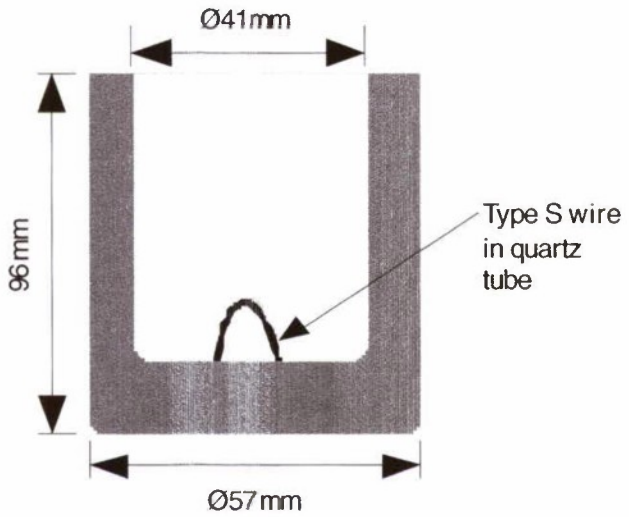

Figure 16 Sketch of TA cup.

Figure 17 TA cup on stand.

RESULTS AND DISCUSSION

1010 EXPERIMENTS

The cooling curves for each experiment were examined to determine the amount of undercooling. Undercooling decreases in the presence of foreign particles that act as heterogeneous nuclei.[2-4,6-7] The reduction results from the fact that the solid/liquid interface does not need to be created. Creation of an interface requires a significant amount of energy and, therefore, driving force. Normally, the driving force for the creation of the interface occurs from the amount of undercooling a liquid melt undergoes before beginning to solidify. The more undercooling a melt experiences the more driving force there is to create the solid/liquid interface. Because the solid/liquid interface is already present, effective heterogeneous nuclei significantly reduce the energy requirement.

There was one complication in the analysis of the steel cooling curves. No recalescence could be detected. It is common practice in other alloy systems to subtract the minimum temperature during recalescence from the liquidus temperature from the cooling curve to determine undercooling.[8-11] Since recalescence was not detected,

the author calculated undercooling by determining the liquidus temperature from the cooling curve and subtracting it from the equilibrium liquidus temperature. The equilibrium liquidus temperature was calculated using the thermodynamic software package Thermo-Calc© and the actual chemical analysis of the steel. Undercooling was then examined relative to the no addition heats on a per powder basis (See Figure 3).

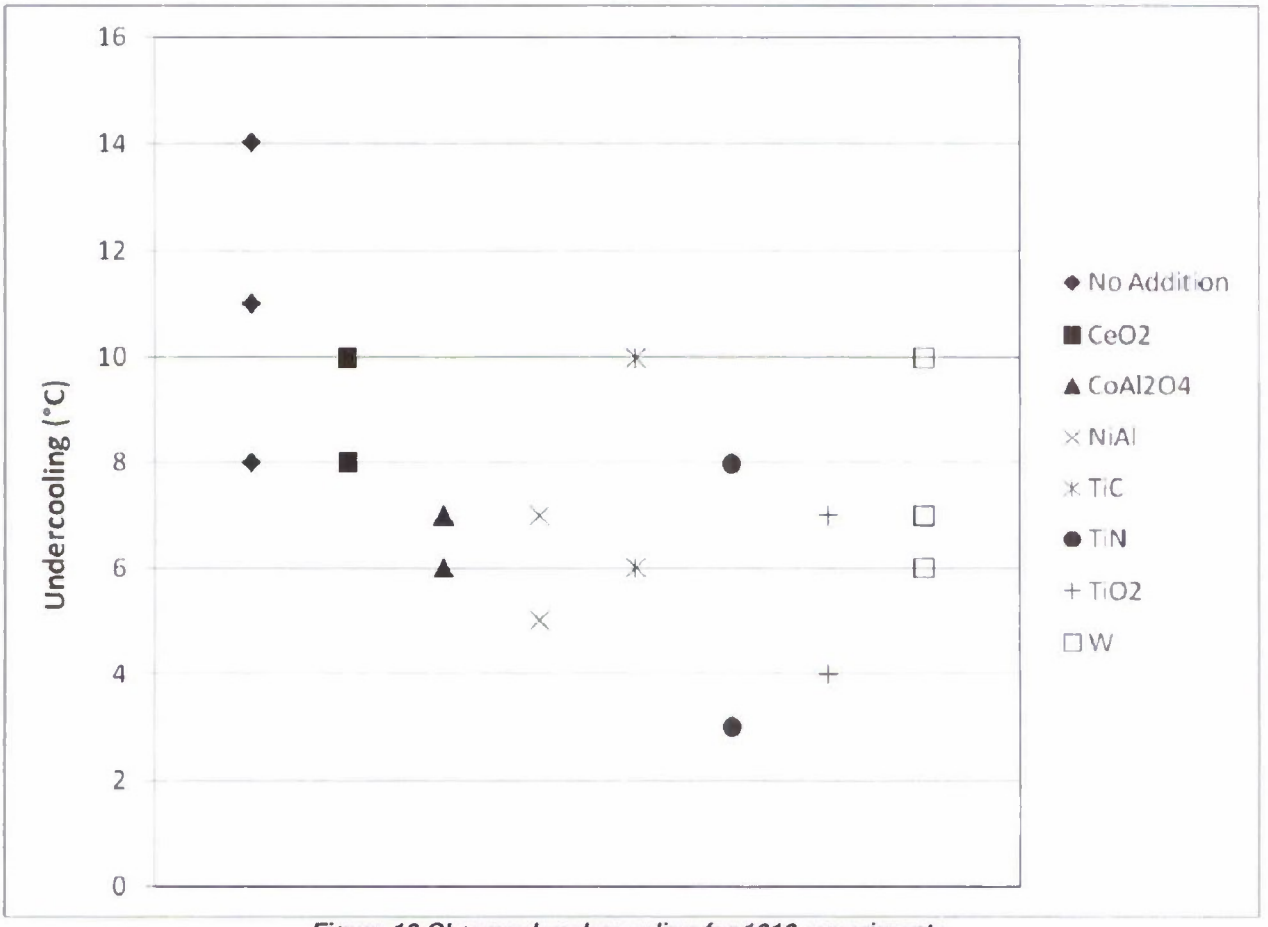

Figure 18 Observed undercooling for 1010 experiments.

$CoAl_2O_4$, NiAl, TiN and TiO_2 produced an observable reduction in undercooling. W and TiC provided a moderate decrease in undercooling. According to other authors, TiN and TiC reduced undercooling.[6] $CoAl_2O_4$ has also been used by investment casting foundries for refining the structure of cast steels.[12] Furthermore, NiAl and W also have excellent crystallographic similarity to δ-ferrite.

The reduction in undercooling by TiO_2 was unexpected. Initially, it was added as a control to ensure that simply adding any particle did not provide refinement. The author originally examined the crystal structure for rutile. Rutile does not have a structure or set of planes that can help nucleate austenite or δ-ferrite. However, the anatase form of TiO_2 was purchased by accident and used in the experiments. Examining the crystal structure of anatase does indicate a possibility. Anatase has a tetragonal crystal structure. Iron atoms could locate on the top or bottom planes (See Figure 4). The distance between the titanium atoms in this structure is close to the cube face diagonals for the BCC structure of δ-ferrite.

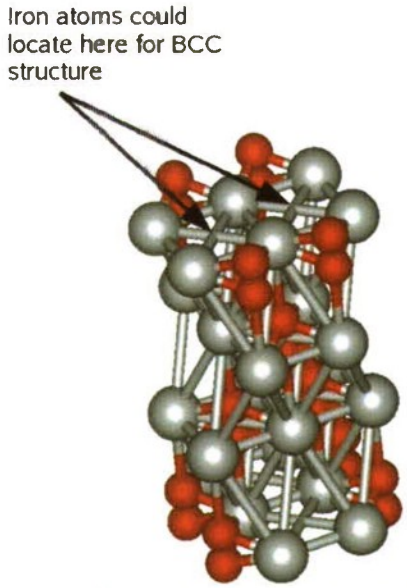

Figure 19 Anatase structure with possible iron atom locations (Ti is gray, O is red).

Iron atoms taking the positions depicted in Figure 4 would explain the reduction in undercooling. This might also explain why Jackson was not able to reproduce the grain refinement he observed in the contaminated FeCr.[13] If he used the rutile form of TiO_2 in subsequent experiments, then he would not have produced a refinement effect.

Interpreting the as-cast microstructures proved difficult. The microstructure consisted of ferrite grains and pearlite colonies (See Figure 5). No discernable reduction in any of the microstructural features could be identified (See Figures 6-13).

Figure 20 Micrograph of 1010 with no addition.

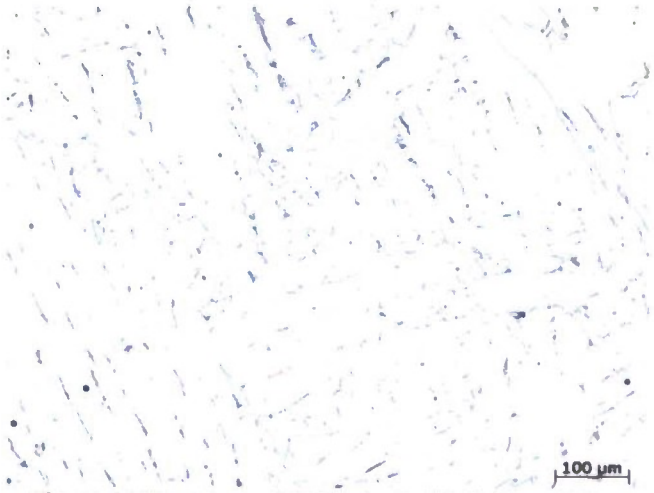

Figure 21 Structure of 1010 steel with CeO_2 addition.

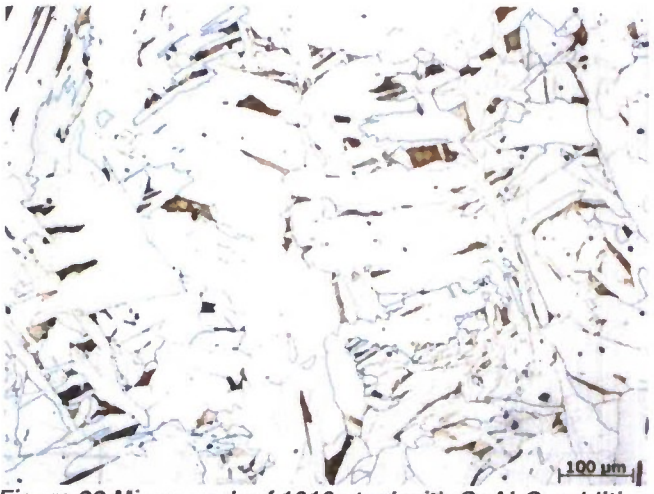

Figure 22 Micrograph of 1010 steel with $CoAl_2O_4$ addition.

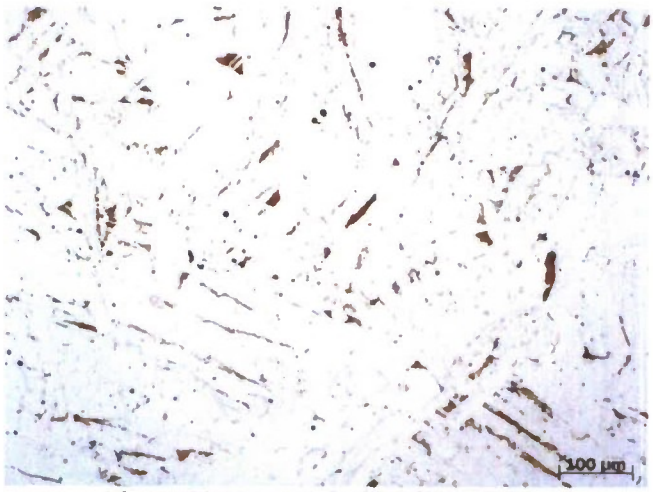

Figure 23 1010 steel with NiAl addition.

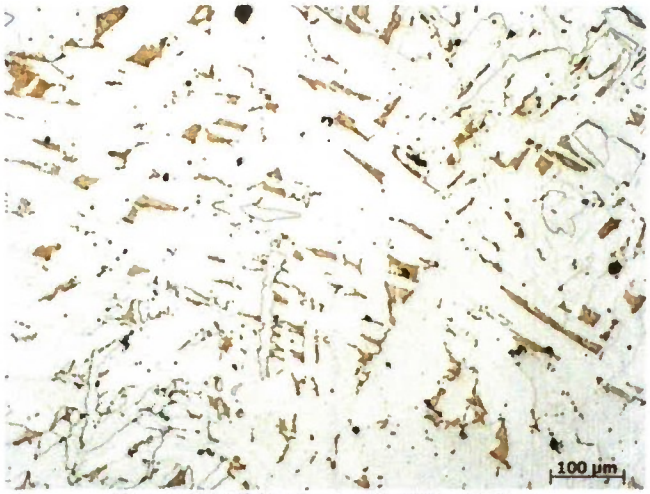

Figure 24 1010 steel with TiC addition.

Figure 25 Micrograph of 1010 steel with TiN added.

Figure 26 1010 steel with TiO_2 powder addition.

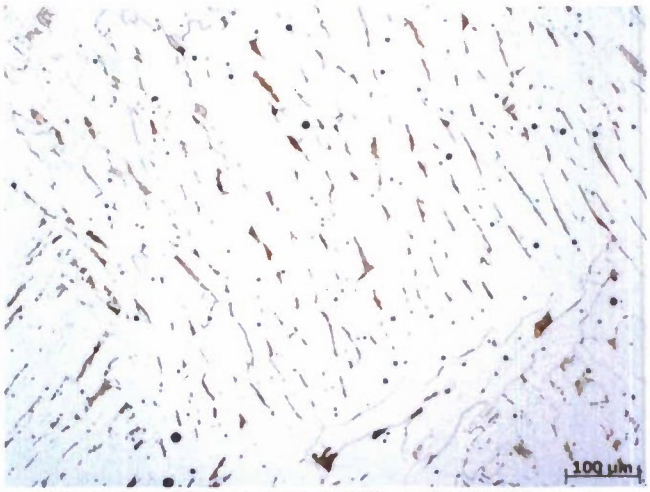

Figure 27 Micrograph of ZrO_2 added 1010 steel.

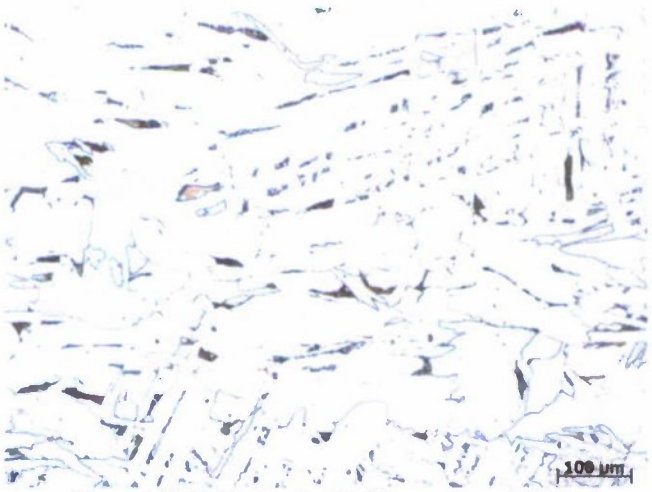

Figure 28 1010 steel with W powder addition.

The lack of detectable refinement in the microstructure was surprising. A possible explanation for these results is that the cooling rate is so rapid in the TA cup that there is a large driving force to nucleate ferrite grains once the eutectoid temperature is reached. All of the micrographs in Figures 5 thru 13 have a ferrite grain size that is similar, but still relatively fine. Ferrite nucleates at austenite dendrite boundaries and other microstructural defects.[13] The rapid cooling rate causes most of the nucleation sites within the material to activate and grow ferrite grains. A large number of grains are created which causes a small ferrite grain size. As the casting cools, ferrite grain growth would occur. This grain growth was limited due to the rapid cooling rate so the fine ferrite size was preserved at room temperature. Such a situation would also occur in castings produced through the shell mold or investment casting routes. It is well known that castings produced through both processes have finer structures due to their higher cooling rates. In fact, this may indicate that grain refinement may not be as important in these processes.

1030 EXPERIMENTS

The amount of undercooling for each powder was recorded (See Figure 14). NbC, and MgO reduced undercooling. AlN, CeO_2 and La_2O_3 provided a small reduction in undercooling. The undercooling reduction by AlN, NbC, and MgO were expected due to their crystallographic similarity to austenite. The reduction in undercooling by CeO_2 was a surprise.

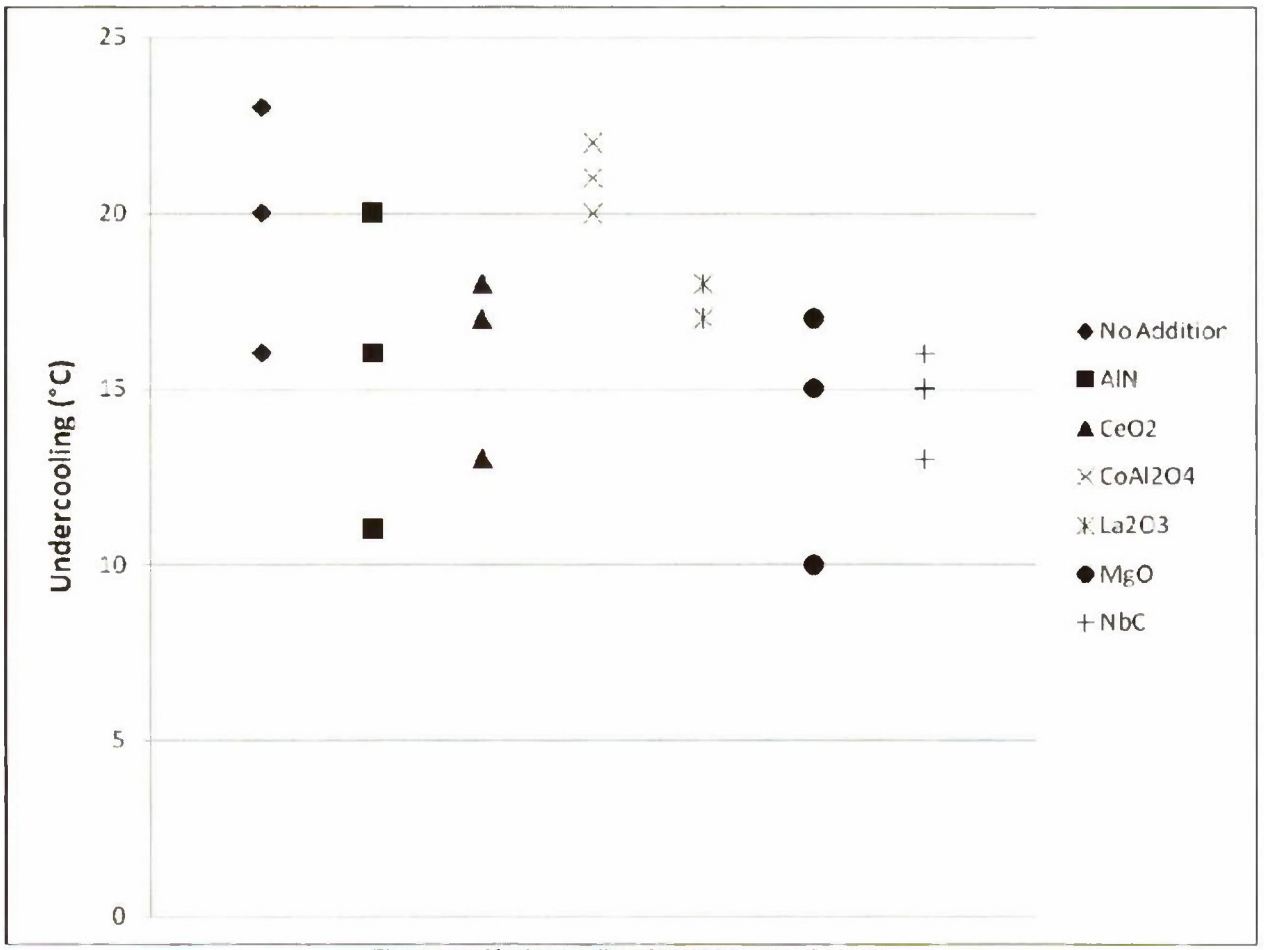

Figure 29 Undercooling for 1030 experiments.

Li at al. observed a similar reduction in undercooling when using CeO_2 additions in the magnetic drop levitation experiments.[14] These authors also found a reduction in undercooling when cerium additions were added to 1045 steel. A solid single crystal layer surrounded the dendritic center of the levitation droplet. CeO_2 particles were discovered in this single crystal layer. When cerium was added to the 1045 steel, CeO_2 and Ce_2O_3 oxides resided in this layer. Oxides were not observed in the dendritic center. The lack of oxides in the dendritic zone, which was refined with the addition of cerium or CeO_2, was not compatible with heterogeneous nucleation theory.[14] Therefore, they attributed the undercooling reduction to a decrease in surface energy and the unique solidification conditions in their experiment.[14] Furthermore, ingot casting experiments did not find any reduction in grain size through the addition of cerium or CeO_2.[14] Other authors have focused on Ce_2O_3 for producing refinement because of its excellent crystallographic match with austenite.[15,16] Ce_2O_3 has also been cited as more stable than CeO_2 which is perhaps why so many researchers have focused on it.[15,16,17]

A cursory examination of the CeO_2 structure indicates that it should not be able to act as a heterogeneous nucleating site for austenite. While the cerium atoms are arranged in a FCC structure, the lattice parameter is 0.5404 nm, much larger than the 0.3648 nm for austenite. Closer examination of the structure does indicate a possible way for CeO_2 to assist austenite nucleate (See Figure 15). If iron atoms are able to enter the space between cerium atoms on the cube edges, then the cube face of the austenite unit cell would be created. This situation provides excellent crystallographic similarity and would explain the observed undercooling reduction in both the current work and Li et. al.'s research.

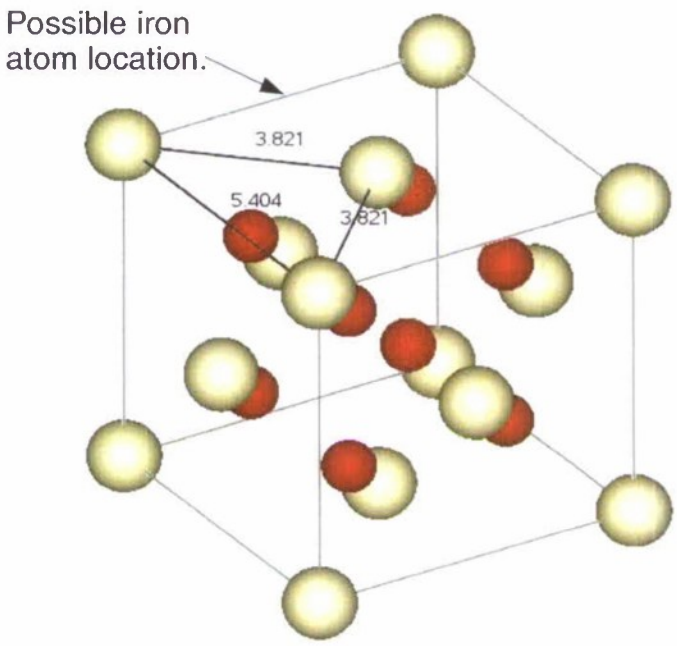

Figure 30 CeO_2 structure with possible iron location (White atoms are Ce, Red atoms are O).

Figure 31 1030 steel with no addition.

Figure 32 1030 steel with AlN addition.

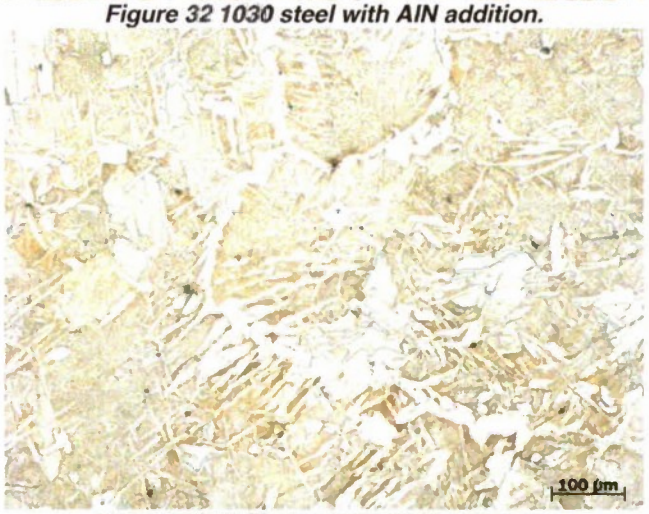

Figure 33 1030 steel with CeO_2 addition.

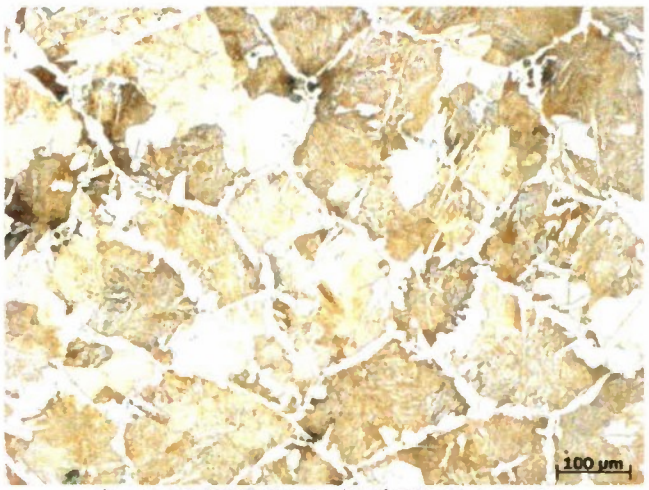

Figure 34 1030 steel with $CoAl_2O_4$ powder.

Figure 35 1030 steel with La_2O_3 addition.

Figure 36 1030 steel with MgO powder addition.

Figure 37 1030 steel with NbC powder.

The final microstructure of the samples consisted mainly of proeutectoid ferrite and pearlite (See Figures 16 through 22). Most of the proeutectoid ferrite was distributed along prior austenite grain boundaries. The delineation of prior austenite grain boundaries makes interpreting these microstructures much easier

than the 1010 samples. In some of the structures, acicular ferrite is observed within the prior austenite grains (See Figures 17, 18, 20, and 22). Formation of the acicular ferrite was due to the high cooling rates involved with the TA samples. Ferrite will nucleate at prior austenite grain boundaries and grow into austenite grains.[13] The observed acicular ferrite probably formed along regions of low carbon concentration. At slower cooling rates, sufficient time is provided for the carbon to diffuse through the microstructure and help form a pearlitic structure within the prior austenite grain.[13] With the relatively high cooling rates of the TA cup, there was insufficient time for this carbon diffusion.

A variation in austenite grain size from the center to the interior of all samples occurred. This was likely caused by the higher cooling rate at the exterior of the sample driving the formation of a large number of austenite dendrites. Figure 16 was from this region because the prior austenite grains were too large to be imaged at the 100X magnification used. The author decided that the reader would have a better idea of the microstructure in the no addition sample if Figure 16 included at least one prior austenite grain. The remaining images were taken from the center of the samples. Grain size reduction is observed for all the materials except La_2O_3. With the exception of the $CoAl_2O_4$ sample, this was expected based on the crystallographic similarity and reduction in undercooling observed. NbC and $CoAl_2O_4$ provided the largest grain size reduction.

The dramatic decrease in prior austenite grain size observed in Figure 22 might be explained by a synergistic effect between NbC particles and Nb dissolved in the liquid melt. Thermodynamic predictions using Thermo-Calc© showed that NbC is not stable in a 1600°C steel melt. However, there is no indication of how fast the decomposition would occur. Since the NbC powder was not in the liquid steel until the steel was poured into the cup, the NbC particles were not in the liquid long before solidification began. If some of the particles dissolved then locally, the melt becomes enriched with Nb and C.

Work in aluminum alloys has found that the presence of a strongly segregating alloying element can assist nucleation and grain refinement.[18, 19] The explanation for this is that the strongly segregating element causes a massive amount of constitutional undercooling which creates a strong driving force for nucleation. Also, the segregation limits the growth of dendrites, reduceing the as-cast grain size. To account for this effect and the effect of the thermal gradient on nucleation, researchers have proposed using the growth restriction factor (GRF).

$$GRF = mC_0(k-1) \qquad \text{Equation 2}$$

where m = the thermal gradient in the liquid, C_0 = the concentration of the solute in the alloy, and k = the equilibrium partition coefficient. The equilibrium partition coefficient can be calculated from the appropriate binary phase diagram by

$$k = \frac{C_s}{C_l} \qquad \text{Equation 3}$$

where C_s = the composition of the solid, and C_l = the composition of the liquid. k can vary with temperature for a particular alloy system.[18,19] However, because it does not typically vary by a large amount an average k value is used for many applications. The partition coefficient for Nb in iron is approximately 0.13, indicating a strong amount of segregation. In addition, the partition coefficient for C is around 0.003. Therefore, dissolution of NbC particles provides two strongly segregating elements which would assist heterogeneous nucleation.

The situation for AlN is different. Thermodynamic calculations also predict that this particle would dissolve in a 1600°C steel melt. However, the partition coefficient for aluminum is 0.81. This is not as strongly segregating as the case for Nb and C. Therefore, the GRF would be smaller, and a coarser microstructure forms (See Figure 17).

ROLE OF COBALT ALUMINATE

$CoAl_2O_4$ produced very different results in the 1010 and 1030 TA experiments. In 1010, it significantly reduced undercooling, but did not in 1030. $CoAl_2O_4$ drastically decreased the prior austenite grain size in 1030 (Refer to Figure 19). It is unfortunate that no observable refinement was produced for any of the 1010 samples. This would certainly have helped determine what role $CoAl_2O_4$ played in both steels.

Other researchers have observed refinement with cobalt aluminate.[20,21] Their work has been using $CoAl_2O_4$ as an interior paint for superalloy investment castings. The alloys examined solidified primarily as austenite. These findings are in agreement with those observed in this paper. No measurements were taken for the undercooling.

Fang et. al. conducted an X-ray diffraction (XRD) study of the $CoAl_2O_4$ coating from investment casting molds after preheating and after pouring.[20] The coating after pouring contained both $CoAl_2O_4$ and metallic cobalt. Cobalt is an FCC metal with a lattice parameter of 0.3565 nm. Therefore, it has excellent crystallographic match with austenite. It is this decomposition product, not $CoAl_2O_4$ itself, which is thought to nucleate austenite. Fang also mixed $CoAl_2O_4$ with Cr, Al, Ti, and C in another set of experiments. The powder mixture was placed in a vacuum differential thermal analysis (DTA) machine which heated them to 1200°C. Once cooled the specimens were investigated with XRD again. In all the specimens, metallic cobalt was found in addition to the original powders. Fang proposed the following reactions for the reduction of $CoAl_2O_4$ based on these results.

$$3\,CoAl_2O_4 + 2\,Cr \rightarrow Cr_2O_3 + Co + Al_2O_3 \qquad \text{Equation 4}$$

$$3\,CoAl_2O_4 + 2\,Al \rightarrow 4\,Al_2O_3 + Co \qquad \text{Equation 5}$$

$$2\,CoAl_2O_4 + Ti \rightarrow TiO_2 + Co + Al_2O_3 \qquad \text{Equation 6}$$

$$CoAl_2O_4 + C \rightarrow CO + Co + Al_2O_3 \qquad \text{Equation 7}$$

Equations 5 and 7 could occur in the 1030 steel produced in this work.

The one unexplained result for $CoAl_2O_4$ is the different undercooling behavior found. Cobalt aluminate reduced undercooling in the 1010 experiments but not in the 1030 experiments. Yet, refinement was observed in 1030. Fang et. al. noted an exothermal reaction at 934 °C which they attributed to the formation of metallic cobalt particles.[20] The heat of formation for a reaction with aluminum was estimated to be -294 kJ, which agreed with the DTA observations.[20] It is possible that this energy release caused the observed reduction in undercooling in the 1010 experiments. Such a release of energy could have kept the temperature of the alloy higher than the case of no addition. Since the liquidus temperature of 1030 is lower than 1010, it is also possible that the $CoAl_2O_4$ powder released its heat of formation at a temperature higher than the liquidus of 1030 preventing the formation of austenite crystals on the metallic cobalt particles. To overcome this energy barrier, the liquid had to undercool more than was observed for the other nucleating phases in this work.

CONCLUSIONS

Several heterogeneous nuclei were found for 1010 and 1030 steel. $CoAl_2O_3$, NiAl, TiN, and TiO_2 reduced undercooling for 1010 steel. The anatase form of TiO_2 was added which may have the ability to

nucleate δ-ferrite. In 1030, AlN, NbC, and MgO reduced undercooling as expected from their crystallographic similarity with austenite. NbC and $CoAl_2O_3$ produced very fine prior austenite grains. Some of the NbC particles may dissolve within the liquid steel, allowing dissolved Nb and C to restrict the grain growth of the growing austenite dendrites. Such growth restriction helped reduced the final as-cast grain size. The energy given off while $CoAl_2O_4$ decomposes to metallic cobalt and other oxides could explain the inconsistent undercooling behavior found. Metallic cobalt provides an excellent nucleation site for austenite which likely assisted austenite nucleation.

REFERENCES

1. Easton, M., and St. John, D. H., *Metallurgical and Materials Transactions A*, volume 30A, pp. 1613-1623A (June 1999)
2. Zhang, M.X., Kelly, P. M., Qian, Ma, Taylor, J. A., *Acta Materialia*, volume 53, issue 11, pp. 3261-3270 (2005)
3. Lee, Y. C., Dahle, A. K., St. John, D. H., *Metallurgical and Materials Transactions A*, volume 31A, issue 11, pp. 2895-2906 (2000)
4. Thomson, J. P., Sadayappan, M., Sahoo, M., *Transactions of the American Foundry Society*, volume 111, pp. 417-434 (2003)
5. Spittle, J. A., Sadli, S., *Materials Science and Technology*, volume 11, issue 6, pp. 533-537 (1995)
6. Bramfitt, B., *Metallurgical Transactions*, volume 1, pp. 1987-1995 (July 1979)
7. Gruzleski, J. E., "Microstructure Development During Metalcasting", American Foundry Society, Schaumburg, IL (2000)
8. Kori, S. A., Rajan, T. P. D., Murty, B. S., Chakraborty, M., *Indian Foundry Journal*, volume 46, issue 8, pp. 35-40 (2000)
9. Gloria, D., Gruzleski, J. E., *Transactions of the American Foundrymen's Society*, volume 107, pp. 419-424 (1999)
10. Johnsson, M., *Thermochimica Acta*, volume 256, issue 1, pp. 107-121 (1995)
11. Closset, B., Pirie, K., Gruzleski, J. E., *Transactions of the American Foundrymen's Society*, volume 92, pp. 123-133 (1984)
12. Ranko, Z., Dracinja, M., Aleksandar, M., *Practical Metallography*, volume 19, pp. 301-317 (1988).
13. Jackson, W.J., *Iron and Steel*, volume 45, issue 2, pp. 163-172 (1972)
14. Li, H., McLean, A., Rutter, J.W., and Sommerville, I.D., *Metallurgical Transactions B*, volume 19B, pp. 383-395 (1988)
15. Qingxiang, Y., Xuejun, R., Bo, L., Mei, Y., and Xin, W., *Journal of Rare Earths*, volume 17, issue 4, pp. 293-297 (1999)
16. Guo, M., and Suito, H., *ISIJ International*, volume 39, issue 7, pp. 722-729 (1999)
17. Wauby, P.E., *International Metals Reviews*, volume 23, issue 2, pp. 74-99 (1978)
18. Easton, M., and St. John, D. H., *Metallurgical and Materials Transactions A*, volume 30A, pp. 1613-1623A (1999)
19. Easton, M., and St. John, D. H., *Metallurgical and Materials Transactions A*, volume 30A, pp. 1625-1633A (1999)
20. Fang, J., and Yu, B., *Proceedings of the High Temperature Alloys Gas Turbines Conference*, pp. 987-997 (1982)
21. Wenzhong, J., Fudong, B., Tingju, L., Guoamo, Y., *Materials Letters*, volume 62, issue 10-11, pp. 1585-1588 (2008)

REPORT DOCUMENTATION PAGE

Form Approved
OMB No. 0704-0188

1. REPORT DATE *(DD-MM-YYYY)*	2. REPORT TYPE	3. DATES COVERED *(From - To)*
27-09-2011	Performance/Technical Reports for FY 2009	01-07-2008 - 30-06-2009

4. TITLE AND SUBTITLE
Solidification Based Grain Refinement in Steels

5a. CONTRACT NUMBER
N00014-08-1-1052

5b. GRANT NUMBER
N00014-08-1-1052

5c. PROGRAM ELEMENT NUMBER

6. AUTHOR(S)
Tuttle, Robert

5d. PROJECT NUMBER

5e. TASK NUMBER

5f. WORK UNIT NUMBER

7. PERFORMING ORGANIZATION NAME(S) AND ADDRESS(ES)
Saginaw Valley State University
7400 Bay Road
University Center, MI 48710

8. PERFORMING ORGANIZATION REPORT NUMBER

9. SPONSORING/MONITORING AGENCY NAME(S) AND ADDRESS(ES)
ONR Reg. Office Chicago - N62880
230 South Dearborn, Room 380
Chicago, IL 60604-1595

10. SPONSOR/MONITOR'S ACRONYM(S)
ONR

11. SPONSORING/MONITORING AGENCY REPORT NUMBER

12. DISTRIBUTION AVAILABILITY STATEMENT
Approved for Pubic Release; distribution is Unlimited

13. SUPPLEMENTARY NOTES

14. ABSTRACT
The overall research objective of this project is to determine suitable grain refiners for cast steels. Specific objectives are:
1) Identify possible phases to grow delta ferrite and austenite using current nucleation theory, crystallographic data, and thermodynamics.
2) Experimentally verify the effectiveness of possible nucleating compounds.
3) Extend grain refinement theory and solidification knowledge through experimental data.
4) Determine structure property relationships for the examined grain refiners.
5) Formulate processing techniques for using grain refiners in the steel casting industry.

15. SUBJECT TERMS
steel, casting, foundry, grain refinement, mechanical properties, solidification, and heterogeneous nucleation

16. SECURITY CLASSIFICATION OF:			17. LIMITATION OF ABSTRACT	18. NUMBER OF PAGES	19a. NAME OF RESPONSIBLE PERSON
a. REPORT	b. ABSTRACT	c. THIS PAGE	UU	18 double-sided pages + SF298	Robert Tuttle
u	u	u			19b. TELEPONE NUMBER *(Include area code)* 989-964-4676